Thesis for the Degree of Master of Engineering

Efficient Short-Range Optical Camera Communication with Motion and Selective Capture

by

Shivani Rajendra Teli

Department of Information and Communications Engineering

The Graduate School

Pukyong National University

February 2018

Efficient Short-Range Optical Camera Communication with Motion and Selective Capture

모션및 선택적 캡쳐를 적용한 효율적인 근거리 광카메라 통신

Advisor: Prof. Yeon Ho Chung

by

Shivani Rajendra Teli

A thesis submitted in partial fulfilment of the requirements for the degree of

Master of Engineering

in Department of Information and Communications Engineering,

The Graduate School,

Pukyong National University

February, 2018

Efficient Short-Range Optical Camera Communication with Motion and Selective Capture

A dissertation

by

Shivani Rajendra Teli

Approved by:

_____

Professor Seok Tae Kim,
(Chairman)

_____

Professor Jun Pyo Hong,
(Member)

_____

Professor Yeon Ho Chung,
(Member)

February, 2018

Table of contents

List of Figures

List of Tables

Acknowledgement

First and foremost, I would like to present my utmost gratitude to my supervisor, Professor Yeon Ho Chung, for providing me with the opportunity to pursue the Master's degree in Mobile Transmission Systems (MTS) Laboratory, Pukyong National University, Busan, South Korea. His thorough supervision and appreciable support have enabled me to materialize my objective of successful completion of Master's degree in Korea.

I would like to thank the members of the Office of International Relations and other department offices in Pukyong National University for the facilities and supports given me for the stay in Korea.

I would like to thank and appreciate my colleagues in the MTS laboratory and the other friends I met in Korea for their support given me in one way or another throughout my precious life in Korea.

Last but not least, my sincere love and thanks to my uncle, Prof. Pramod Shendge who recommended me to study in Korea, my mother, father and brother for their words of encouragement and love which brought me faith and a happy life while staying away from home.

Shivani Rajendra Teli

Department of Information and Communications Engineering

Pukyong National University, Busan, South Korea

Efficient Short-range Optical Camera Communications with Motion and Selective Capture

Shivani Rajendra Teli

Department of Information and Communications Engineering, The Graduate School,
Pukyong National University

Abstract

With the advancements in smart device and mobile phone cameras and light emitting diodes (LEDs), optical camera communication (OCC), also termed camera-based visible light communication (CVLC) has emerged as a novel communication scheme for providing data communication. Using visible light, as the communication medium, VLC and OCC possess many advantages over conventional RF communications, such as large unlicensed spectral bandwidth, usability at radio frequency (RF) prohibited areas. The OCC technique is an extension of VLC with the advantage of no extended hardware cost of the receiver in most smart devices. Unlike conventional VLCs, which employ photodetectors (PDs), the OCC utilizes a mobile phone CMOS camera as the receiver. That is, OCC captures two-dimensional (2D) data in the form of image sequences, thus being able to transmit more information compared to photodetector-based VLCs. In order to exploit the applications to provide cost-effective and convenient smart home environments as well as high-speed data communication, this thesis addresses applications and important issues in indoor OCCs. Moreover, the thesis provides a fundamental analysis of the OCC system in aspects of illumination and data rate.

In the first study, a flexible and novel motion detection scheme over a smart device camera in OCC is proposed. The motion detection is performed in conjunction with a static downlink OCC, where a mobile phone front camera is employed as the receiver and an 8×8 dot matrix LED as the transmitter. To provide illumination and communication, additional 10 white LEDs are employed which also helps in acquiring camera focus, and light metering. The motion detection or motion over camera (MoC) is designed to detect the user's finger movement through the OCC link via the camera. A simple but efficient quadrant division based motion detection algorithm is proposed for accurate detection of motion. The experiment and simulation results demonstrate that the proposed scheme is able to detect motion with a success probability of up to 96 percent in the mobile phone camera based OCC. It is envisioned that the proposed motion detection can facilitate cost-effective and convenient smart home environments in the OCC, where the provision of illumination and short-range wireless communications has already been addressed.

Secondly, the thesis presents a novel concept of trained neurons based motion detection (TNMD) in OCC. The TNMD is proposed in order to enhance the performance of the motion detection proposed in the first study for its realistic and practical implementations. The proposed TNMD is based on neurons present in a neural network (NN) that perform repetitive analysis in order to provide efficient and reliable motion detection in OCC. This efficient motion detection can be considered another functionality of OCC in addition to two traditional functionalities of illumination and communication. The motion is detected in the similar fashion as described in the first study, that is, by observing the user's finger movement in the form of centroid through the OCC link via a camera. Unlike conventionally trained neurons

approaches, the proposed TNMD is trained not with motion itself but with centroid data samples, thus providing more accurate detection and far less complex detection algorithm. Experiment results demonstrate that the TNMD can detect all considered motions accurately with acceptable bit error rate (BER) performances at a transmission distance of up to 175 cm. The OCC with the proposed TNMD combined can be considered an efficient indoor OCC system that provides illumination, communication and motion detection in a convenient smart home environment.

The last study in this thesis proposes a distinct capturing strategy called selective capture (SC) in order to achieve high-speed and flicker-free OCC based vehicle-to-vehicle (V2V) communication. In optical camera communication (OCC), much effort has focused on increasing data rate and communication distance by maximally utilizing spatial, frequency, intensity or color dimensions. The major challenge in OCC is low data transmission rate, due to the low sampling rate of a camera-based receiver, compared with high-speed modulation of light emitting diodes (LEDs). Due to the use of the SC technique for capturing the taillights in the form of data frames, the capture speed of RaspiCam is increased from 120 frames per second (fps) to 435 fps, yielding an efficient, high-speed and flicker-free OCC for V2V. The experiment results demonstrate that the proposed OCC for V2V using SC technique achieves acceptable bit error rate (BER) performance at a distance of up to 175 cm.

1. Introduction

1.1 Optical Wireless Communication

Wireless technologies have become essential in everyday life over the last four decades and are expected to be considered a key element of societal progress in the near future. The rapid growth of wireless communication has led to an increase in the demand for advanced ubiquitous mobile applications in people's daily lives. Due to the increasing demands for high-speed data transmission, the wireless system needs to provide gigabit connectivity. It is challenging to provide higher data rates for an increasing number of users using radio frequency (RF) because of its limited availability due to congested spectrum. Therefore, the expansion of RF band towards the optical spectrum is imminent on a commercial scale.

Optical wireless communication (OWC) system is likely to be a part of the future heterogeneous network as a complementary option to RF, and in contention to be featured in fifth generation (5G) network [1][2]. OWC can play a major role to meet the requirements for 5G technology and is expected to extensively change the existing infrastructure by reducing the deployment costs with the introduction of new technologies, such as new Physical layer

(PHY) architectures, data links, network layer functionalities, and interfaces with different service layers [2].

1.1.1 Visible Light Communication

OWC using visible light (VL) spectrum, known as visible light communications (VLC), gained popularity a decade ago. With various advantages such as license-free spectrum, electromagnetic interference-free transmission and, high security, VL is now able to provide a data rate of gigabits per second (Gbps) [3]. The potential of using VL for wireless communication was first demonstrated by transmitting an audio signal using VL in [4]. Therefore, VLC with abundant bandwidth (in terahertz) is emerging as a compelling technology that has potential to change the face of future wireless communications [4]. Considering this, a communication protocol for VLC was proposed in the IEEE standard 802.15.7 [5].

In a VLC system, light emitting diodes (LEDs) are used as transmitters and photodetectors (PDs) as receivers. The VLC system relies predominantly on intensity modulation and direct detection (IM/DD) technique for communication and offers two unique functionalities: illumination and

communication. Another interesting and unique functionality of VLC based motion detection has recently been reported in the literature [6].

Together with other known advantages, such as cost-effectiveness and no harm to humans and electronic devices and use of existing illumination infrastructure, the deployment of VLC systems is envisioned to grow rapidly for years to come. In the area of smart home applications, VLC has also been considered to efficiently support various smart devices [6][7].

1.1.2 Optical Camera Communication

Over the past few decades, Mobile phones and smart devices equipped with a built-in complementary metal oxide semiconductor (CMOS) camera have become pervasive consumer electronics and are being explored to deliver extra capabilities beyond traditional imaging. Along with mobile phone cameras, a majority of smart devices with built-in CMOS cameras provide the ability to capture photos and videos. Current cameras are capable of capturing high-resolution videos with a resolution of at least 1280×720 pixels and a capture rate of 30 fps [8][9]. Considering the capabilities, and increasing demand of cameras a new optical communication technique using a camera as the receiver has been studied in the IEEE 802.15 SG7a within the framework

of OWC and considered as a candidate of IEEE 802.15.7rl, which is termed as optical camera communication [10].

Optical camera communication (OCC) is a pragmatic version of VLC using a camera as the receiver and a light emitting diode (LED) as the transmitter [11]. The OCC can capture 2D data in the form of image sequences; therefore, it can transmit more information compared with intensity level based photodiodes in VLC [9]. A series of images, called frames, captured by the camera contains more information in the form of not only the intensity captured by photodiodes but also multiple colors and spatial coordinates [8][2][8]. Yet OCC suffers from a long processing time of the frames due to a larger dimension of frames and a significantly lower data rate compared with other VLC schemes.

The potential of increasing OCC data rate was investigated in [11] by using an array of LEDs as the transmitter, in order to exploit an advantage of having a 2D space from the captured frames. Recently, cameras with a color filter array over an image sensor have also become very common, due to which the use of red, green and blue (RGB) LEDs as transmitters is possible [12]. The experimental results presented that a single commercially available RGB LED and standard 50-frames per second (fps) camera were able to achieve a data

rate of 150 bits/s over a range of up to 60 m [12]. Another OCC research developed a high data rate of 126.72 kbps by employing a not commercially available high capture rate camera of 330 fps and multiple intensity levels of colors to modulate [13].

1.2 Research Motivations

Recognizing the potential and advantages in OCCs, the following studies were motivated to contribute to the development of a motion detection and selective capture schemes in OCC.

- **Camera-based motion detection techniques:** Motion detection techniques have been studied as optical motion detection [14] and a gesture control technique [15] utilizing infrared beam and camera (webcam) receivers. The drawback of IR based motion detection techniques is that it cannot be used for illumination and communication. To this end, authors introduced motion detection as an additional functionality in VLCs along with to primary functionalities of illumination and communication [6]. The motion detection scheme can be considered attractive and viable for controlling smart devices in future VLC-based smart homes [6][7]. However, the motion detection technique in VLC [6] has unrealistic placement of PDs in smart home applications. To address this issue and by considering the availability and capabilities of the cameras as the receiver, a camera-based motion detection is considered in OCC. This technique offers a convenient and cost-effective motion detection in a smart home environment exhibiting great potential in indoor OCC. Therefore, we

propose a camera-based motion detection as a new paradigm of functionality in OCC, which can be used to control the smart devices in conjunction with existing OCC links [11].

- **Neural network assisted motion detection:** To enhance the performance of the motion detection functionality in OCC [9], we propose a Neural Network (NN) assisted motion detection in OCC. The conventional camera-based motion detection in OCC provided a short-range of motion and communication distance. For practical implementation, it is necessary to enhance the performance of motion detection in terms of accuracy and motion and communication distance. The NN based image and pattern recognition have recently emerged as an efficient detection method [16][17]. The artificial neurons present in the hidden layers of the network are trained to optimize the network in terms of some fundamental criteria such as accuracy and robustness. Due to this, the formation of complex algorithms can be avoided. Motivated by the potential of neuron training, we propose a more practical and realistic camera-based motion detection scheme over an existing OCC link. We consider the fact that the motion performed by the user represents some pattern in the form of shape. Therefore, the performance of motion detection in the OCC can be

improved in terms of accuracy and transmission distance by utilizing the neuron based training.

- **Selective capture for V2V:** The OCC has the advantage of transmitting more data because of its 2-dimension data capturing capability in the form of images due to use of camera receiver [11]. However, due to the low sampling rate of a camera compared with high-speed modulation of light emitting diodes (LEDs), OCC has to suffer from a significantly lower data rate compared with other VLC schemes. The data modulation at the transmitter must provide a wide range of dimming level so as to exhibit no flickering. According to the IEEE 802.15.7 VLC standard, the maximum flickering time period (MFTP) must be 5 ms (200 HZ) so that a typical human eye cannot respond to LED flickering [5]. However, due to the limited camera capturing speed of the 30/60 frames per second (fps), the camera itself can acquire signals at a very low sampling rate resulting in lower data rate. Therefore, we propose a high-speed OCC using a novel capturing strategy called selective capture (SC). The camera receiver is tweaked to capture the selected area only from the full camera capture frame, thus being termed as selective capture (SC). Unlike conventional OCC schemes, the proposed scheme performs the SC in the frame, not

after the frames are captured. A Raspberry Pi camera module (RaspiCam) was used as the receiver was tweaked to capture the SC only. Due to this, the RaspiCam produces a capture speed of 435 fps at a minimum resolution of 640×480 pixels; therefore, the LED flickering rate can be increased up to 217 Hz.

Recently the use of LEDs in traffic applications and the growing interest in intelligent transport systems (ITS) presents a number of opportunities for VLC and OCC applications. The LED traffic lights and LED brake lights can be used for data transmission [18][19]. Many efforts have focused on increasing data rate and communication distance to achieve a useful OCC system for automotive applications. Therefore, we utilized the SC scheme to propose a high-speed and flicker-free OCC for vehicle-to-vehicle (V2V). Due to the use of SC scheme, the RaspiCam installed on the vehicle (V_1) following another vehicle and was tweaked to capture the SC only, i.e., the taillights of the leading vehicle (V_2), thus resulting in a higher data transmission rate in an OCC link. As the RaspiCam captures only the taillights of V_2 excluding the surrounding, therefore, reducing the processing time and increasing the data transmission rate.

1.3 Thesis Objective

With the abovementioned motivations, the study in this thesis considers the following objectives:

i. To propose a cost-effective and convenient smart home environment based on motion detection over the OCC link.

ii. To enhance the performance of the proposed motion detection in OCC in terms of accuracy and robustness using neural networks to propose more practical and realistic implementation of OCC based motion detection.

iii. To address a critical issue of data rate enhancement in OCC by proposing a new capturing strategy called selective capture technique for V2V communication.

1.4 Chapter Organization

The remaining chapters in this thesis are outlined as follows. Chapter 2 describes the overview of the study related to image processing based motion detection and selective capture techniques. The performance of motion detection technique is analyzed in terms of percentage of success over existing OCC links. This camera-based motion detection in OCC is presented in Chapter 3. To enhance the performance of the proposed camera-based motion detection, neural network assisted motion detection is studied in Chapter 4. Chapter 5 presents the distinct capturing strategy called selective capture for high-speed and flicker-free optical camera based V2V communication. Chapter 6 concludes the study considering all the simulations and experiment analysis.

2. Motion Detection and Selective Capture

This chapter of the thesis is based on the image processing as a computer-based technology, which performs automatic processing of visual information. Image processing plays an increasingly important role in many aspects of our daily life, as well as in a wide variety of disciplines and fields in science and technology. Therefore, it is used for various applications such as television, photography, robotics, remote sensing, medical diagnosis and industrial inspection. In this chapter, we focus on the three distinct applications such as motion detection and selective capture.

2.1 Principle of Motion Detection

Motion detection is a process of detecting the change in the movement of an object with respect to its surroundings or a change in the surroundings with respect to an object. Motion can be detected by:

- Infrared (passive and active sensors)
- Optics (video and camera systems)
- Radio frequency energy (radar, microwave and tomographic motion detection)
- Sound (microphones, seismic and inertia-switch sensors)

- Magnetism (magnetic sensors and magnetometers)

Over the last few years, an important stream of research within computer vision, i.e., understanding of human activity from a video captured by the camera has gained a lot of importance. This human activity or movement is defined as motion detection. Motion detection is a process of detecting a change in the position of an object relative to its surroundings or a change in the surroundings relative to an object [20]. The principle of motion detection is to recognize the motion of objects within the image frames. The study related to the human motion analysis is strongly motivated by recent improvements in computer vision and a variety of new promising applications such as personal identification and visual surveillance. In video surveillance, motion detection refers to the capability of the surveillance system to detect motion and capture the events. Motion detection is usually a software-based monitoring algorithm, which, when it detects motions will signal the surveillance camera to begin capturing the event. Also called activity detection. The motion analysis related to the human body is an interesting research due to its various applications such as physical performance, evaluation, medical diagnostics and virtual reality.

Intelligent video sensors were developed to support security systems to detect unexpected movement without human intervention [23]. The important information of move, location, speed and any desired information of target from the captured frames can be taken from the camera and can be transferred to the analysis part of the system. Movement detection is one of these intelligent systems which detect and tracks moving targets. The well-known methods used in moving object detection are the frame subtraction method, the background subtraction method, and the optical flow method [22]. The optical flow method calculates the image optical flow field and performs cluster processing according to the optical flow distribution characteristics of the image. The background subtraction method involves the use of the difference between the current image and background image to detect moving objects. In the frame subtraction method, the moving object is recognized by calculating the difference between two consecutive images.

2.2 Importance of Motion Detection

The motion detection techniques also termed gesture recognition is studied widely in the field of image processing. It is defined as the process by which the gestures made by the user are recognized by the receiver [20]. Gestures are

expressive, meaningful body motions involving physical movements of the fingers, hands, arms, head, face or body. These gestures are the meaningful body motions that can convey meaningful information or help to interact with the environment. There are various approaches to handle the motion gesture recognition such as soft computing, various mathematical models and different imaging and tracking techniques [20]. Gesture recognition has wide-ranging applications [20] such as follows:

- Developing aids for the hearing impaired.
- Designing techniques for forensic identification.
- Recognizing sign language.
- Medically monitoring patients' emotional states or stress levels.
- Lie detection.
- Communicating in video conferencing.
- Tele-teaching assistance.
- Monitoring alertness/drowsiness levels for automobile drivers.

Various computer vision and pattern recognition techniques including feature extraction, object detection, clustering, and classification are used for many gesture recognition systems [21]. Image processing techniques [22] such

as analysis of shape, color, texture, motion, image enhancement and segmentation play an important role in motion gesture recognition.

Authors proposed a gesture control scheme to control the mouse cursor of a personal computer using single web camera as an input device to recognize the gestures of hand [23]. This scheme detects the gestures by scanning the peak of a user's fingers using web camera and controls the mouse cursor. The advent of Kinect has made efforts to apply gesture control not only in gaming, but rather in controlling TVs or set-top boxes, PCs, laptops, and others [14]. A similar study based on gesture control technique using infrared (IR) beam was investigated in [14]. In late 2008, a new way of interacting with computers was demonstrated using 3D IR camera and OpenCV in order to make computers understand gestures represented by hands and finger movements [14][23]. The technology adopted by Microsoft from Prime Sense established a new stage in the evolution of man-computer interaction. The motion detection was also proposed as human sensing using VLC in [24] and was introduced as a new additional functionality in VLC along with illumination and communication in [6]. However, the motion detection in PD based VLC scheme lacks the practical and realistic placement of PDs. The concept of motion detection can be further studied as attractive and viable controlling

technique to control the smart devices in future VLC-based smart homes [6][7]. Considering this, we try to implement the motion detection using mobile phone camera over the existing OCC links to provide convenient smart home environments in OCC with three functionalities of motion detection, illumination, and communication.

2.3 Selective capture

Recently, the concept of region-of-interest (ROI) is studied to extract the interested region or the information from the captured (source) image. In terms of image processing, ROI is defined as a portion of an image that is filtered to perform some other operations on [25] as shown in Figure 2.1. The ROI can also be defined as the samples within a dataset identified for a particular purpose. The various examples of ROI are listed as follows:

- 1D dataset: time or frequency interval on a waveform.
- 2D dataset: boundaries of an object on an image.
- 3D dataset: contours or surfaces outlining an object in a volume.
- 4D dataset: outline of an object during a particular time interval in a time-volume.

In terms of ROI-based processing, the ROI can be defined by creating a binary mask, which is a binary image with the same size as the image to be processed. In the mask image, the pixels that represent the ROI are set to 1 while all other pixels are set to 0. Multiple ROIs can be defined in an image. These regions can be geographic in nature, such as polygons that contains contiguous pixels or defined by a range of intensities. However, the pixels are not necessarily contiguous in all the cases.

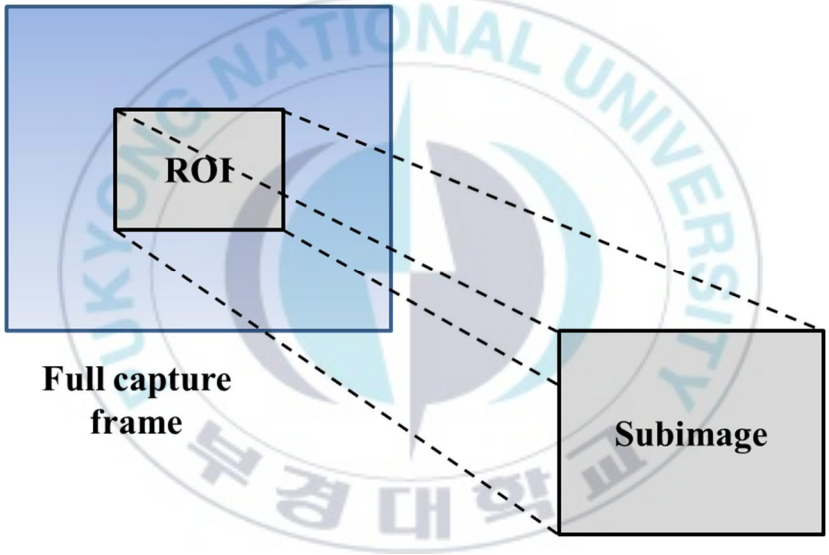

Figure 2.1. The concept of Region-of-interest.

Authors utilized this ROI for various intelligence, surveillance, and reconnaissance applications to detect potential targets or ROIs in digital imagery [25]. The ROI can be used to automatically call for further sensing,

to control intelligent image-compression algorithms or to direct further analysis for target identification and recognition. Most ROI detection based algorithms use feature-based or object-based approaches. The ROIs formed using feature-based methods find pixels that share significant optical features with the target. While object-based methods detect ROIs at a higher level than the pixel-by-pixel approach of feature-based systems by using information such as target shape and structure. The template matching and matched filters are the typical approaches included in the object-based ROI detection methods.

The study in [26] listed the Region-of-interest Sub-sampling as one of the sampling methods that can be employed for OCC so as to increase the camera frame rate significantly. The scheme in [27] describes the CCD camera hardware modification utilizing a Texas Instruments TC237 CCD imager chip with sub-frame window read out. However, the study utilizing the ROI Sub-sampling by modifying the image sensor as mentioned in [25] for OCC is not yet implemented.

To this end, authors implemented a full high-speed OCC scheme using a similar technique called as selective capture [27]. The proposed selective capture scheme is based on software tweaking of the camera receiver to capture the selected area only from the full camera capture frame. Therefore,

it is termed as selective capture (SC). Unlike conventional OCC schemes, the proposed scheme performs the SC in the frame, not after the frames are captured. A Raspberry Pi camera module (RaspiCam) is used as the receiver and was tweaked to capture the SC only, thus resulting in a higher data transmission rate in an OCC link. The Linux commanding tool is used to tweak the RaspiCam to selectively capture the selected area from the full capture frame. The capture parameters such as the recording time of the video, the resolution at which the video is to be captured and the SC area is set using the Linux commanding tool. The details of the SC scheme are described in the subsequent sections.

3. Camera-based Motion Detection Techniques

The target of this study is to develop a cost-effective and short-range OCC for convenient smart home environments using motion detection techniques as mentioned in Chapter 2. A flexible and novel motion detection scheme over a smart device camera in OCC is developed. Therefore, three independent functionalities are provided from the existing OCC links, i.e., illumination, communication and motion detection. We also propose an algorithm to identify the motion performed by the user. To verify the effectiveness of the proposed system, experiments and simulations were performed in the indoor OCC environment.

3.1 Camera-based Visible Light Communication

Over the past few decades, mobile phones have been equipped with a built-in complementary metal-oxide-semiconductor (CMOS) camera. The mobile phones are capable of capturing high-resolution videos with a resolution of at least 1280 × 720 pixels and a capture rate of 30 fps [9][11]. Considering this advantages and availability of cameras, camera-based VLCs (CVLCs) have recently emerged [10][11]. A mobile phone CMOS camera is utilized as a

receiver instead of photodiodes to capture data from the transmitting LEDs as shown in Figure 3.1.

The advantage of CVLC over photodiode based VLCs is that it can capture 2-D data in the form of image sequences. Therefore, it can transmit more information, compared to the photodiodes based VLCs acquiring only color and intensity. Yet the CVLC suffers from drawbacks such as high-speed processing for detection and recognition of data from the images [28]. In addition to this, cameras have limited capture speed as well as need to deal with focus and light metering to have an optimum identifiable image. The limited frame rate of CVLC was compensated by employing both multiple colors and spatial diversification in an LED array [29]. Authors proposed a scheme that addresses the important issues of CVLC, i.e., focus and capture rate. It provides illumination and offers rotation compensation without significant reduction in data rate [11]. As shown in Figure 3.1, the CVLC scheme employs LED array as transmitter and mobile phone front camera as the receiver. The eight white LEDs are employed for illumination and more accurate camera focus. In [11] 64 LEDs (8×8 LED array) were utilized for data transmission with 20 pulses per second (pps) LED flickering rate (LFR). In CVLC there often exists a discrepancy between camera capture rate (CR) and

LED flickering rate (LFR). The CR in CVLC is viewed as a camera sampling rate, whereas the LFR is a rate at which an LED transmits the data. Moreover, the concept of keyframe (header) to provide the rotation compensation at the expense of slight data reduction is also proposed. The keyframe acts as a header for time and data synchronization [11][19]. The target applications of the CVLC scheme as listed in [11] are to facilitate efficient exhibition and display, where visitors can easily access the information on display items through their smartphone cameras.

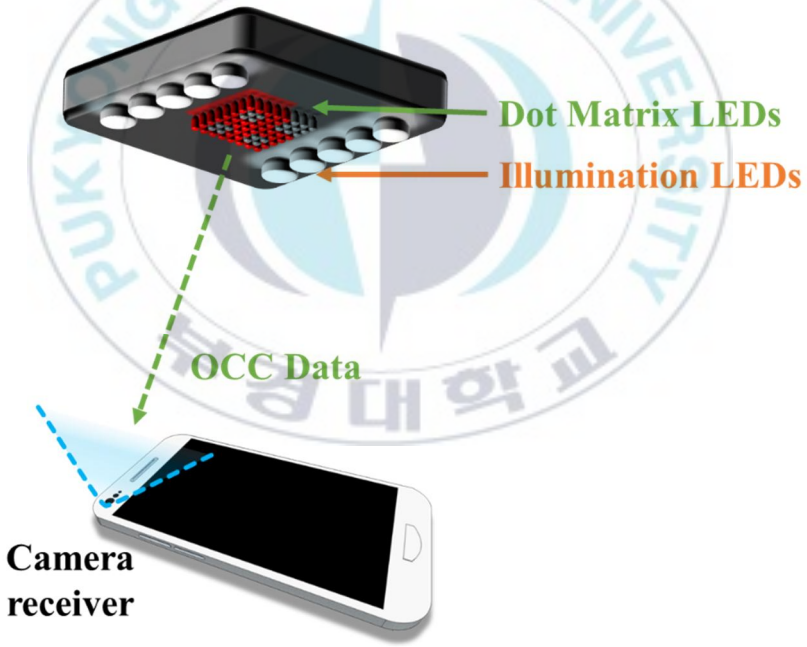

Figure 3.1. Overview of CVLC scheme.

3.2 Motion Detection over Camera in OCC

Considering the various advantages and availability of mobile phone cameras, a new optical communication technique using cameras has been studied in IEEE 802.15 SG7a within the framework of optical wireless communications and considered as a candidate for IEEE 802.15.7rl, which is called optical camera communication (OCC) [10]. OCC increase the potentiality of VLC due to increasing usage of mobile phone cameras that can be used as a receiver without any extra hardware adjustment.

The VLC based motion detection has been introduced as an additional functionality in VLCs along with illumination and communication as two primary functionalities [6]. This Motion detection scheme is deemed attractive for controlling smart devices in future VLC based smart homes [6][7]. However, this VLC based motion detection technique has an unrealistic placement of PDs in smart home applications. Therefore, to overcome this issue, we proposed a simple and convenient mobile phone camera based motion detection or motion over camera (MoC) technique along with communication in the OCCs. The motion detection is considered to provide

an additional functionality to the OCC with two traditional functionalities of illumination and communication.

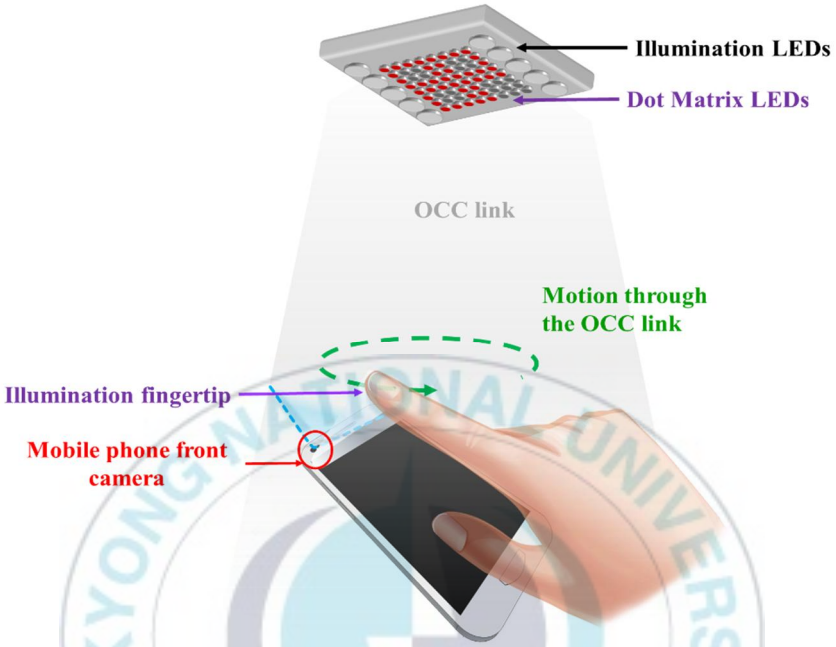

Figure 3.2. System overview.

In the proposed technique, MoC is carried out by monitoring the movement of user's finger captured in the front camera of the mobile phone. This captured movement of user's finger is then processed to identify and detect the motion performed by the user through the OCC link. Figure 3.2 shows the overview of proposed MoC in OCC. An 8×8 dot matrix LED is used as a transmitter and ten white illumination LEDs are placed over the dot matrix LED for both

illumination and a reference for camera light metering and focus [11]. These illumination LEDs also help to illuminate the user's finger as the illumination strikes the mobile phone screen and is reflected back towards the finger as shown in Figure 3.2. This illumination assists the tracking of motion because it provides a clearer distinction between the finger and its surrounding.

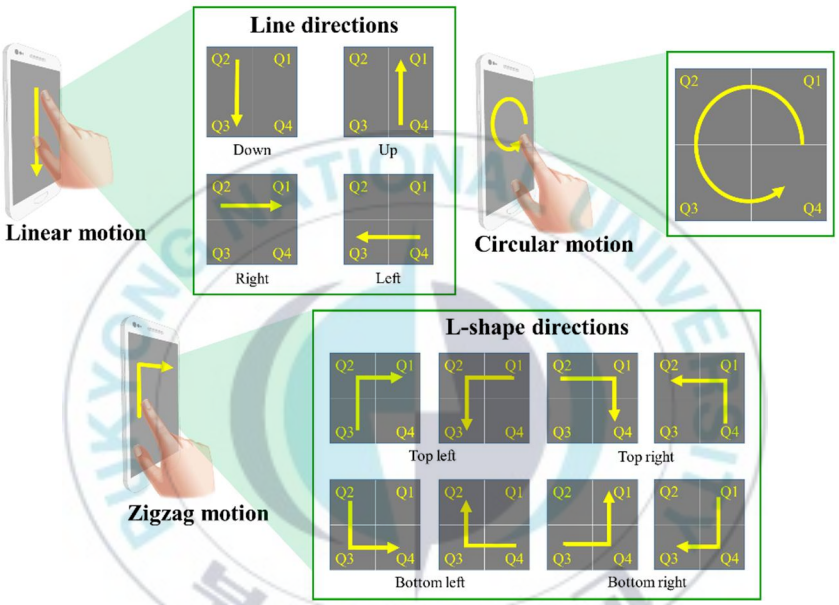

Figure 3.3. Three motions: line, L-shape, and circle.

The user is required to make the motion over the camera of his mobile phone placed under the dot matrix LED in a static condition for more realistic control. This motion is captured by the mobile phone camera in the form of a video, which is then split into various frames for processing. We designed the

quadrant division based motion detection algorithm for the processing of the frames. The predefined motions: line, L-shape, and circle motions are chosen based on the simplicity and flexibility that the user can easily and naturally perform. Figure 3.3 shows these three predefined motions. The figure also shows the possible directions for the line motion and L-shape motions that can be detected by the proposed algorithm.

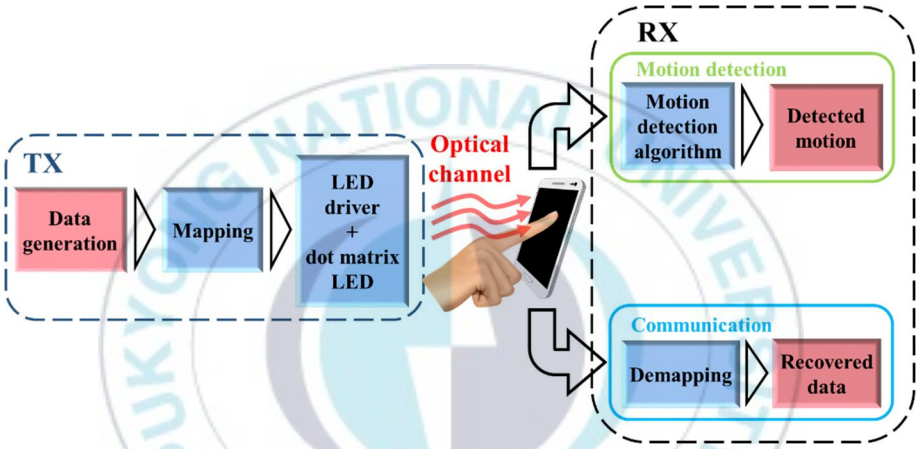

Figure 3.4. Block diagram of the proposed scheme.

The block diagram of the proposed MoC in the OCC is illustrated in Figure 3.4. The transmitter comprises the data generation block which generates random data for transmission along with its keyframe. The keyframe is a special header frame introduced in generated data for evaluating the transmitted data on the receiver side [11][19]. The most commonly used on-

off keying (OOK) modulation was employed for the data modulation in OCC to transmit data, through each LED of the 8×8 dot matrix LED array [11]. The mapping block maps the data according to the LED array addresses. The mapped data is then passed on to the LED driver for OCC transmission through dot matrix LED.

On the receiver side, the mobile phone camera is used both for motion detection and OCC data reception. Along the OCC link, the motion is performed by the user's finger. For the motion detection algorithm, the key function is to compare changes between received frames from the mobile phone camera. The changes are expressed in the form of centroids that represent the centre of a moving object in terms of the coordinate. The detected centroids are then fed to the motion detection algorithm, where the distribution of centroids is analyzed and the motion is identified. Simultaneously on the OCC link, a demapping process performs time as well as spatial synchronization to detect keyframe and extract data from the received frames. The proposed OCC link uses differential detection threshold (DDT) to detect each LED in the array [11].

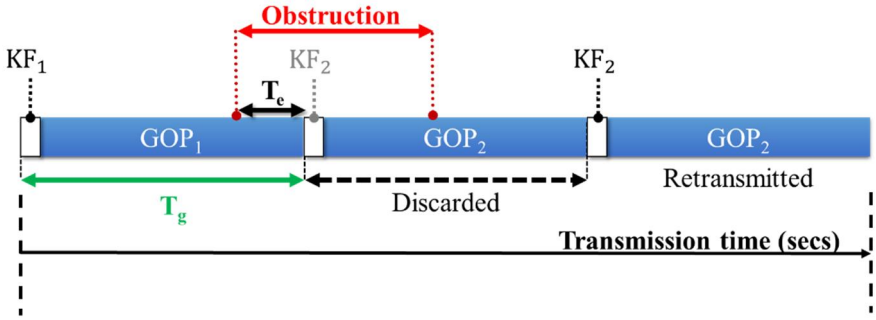

Figure 3.5. Keyframe configuration.

As previously mentioned, a keyframe is added periodically on the transmitter side as a header between every group of pictures (GOP), which is a term that represents a group of data frames. This keyframe is added as a header for data synchronization, through which it compensates for data loss by repeat request when the link is obstructed due to the motion. The keyframe reduces the data transmission rate slightly because it takes one time-slot in the beginning of GOP. The duration of the keyframe and GOP, denoted as T_g. when the obstruction due to motion occurs as shown in Figure. 3.5, some part of GOP_1 (T_e), KF2 and part of GOP_2 will be obstructed, causing bit errors in the received data. As the keyframe KF_2 is not detected in the receiver, the most recent GOP (i.e., GOP_2) will be discarded and retransmitted via the receiver's repeat request. Due to this, the data of GOP_2 will eventually be recovered. In the present study, the data over T_e period is lost and is not compensated. The

data loss can be reduced by reducing T_g as a shorter T_g would, however, decrease the data rate. Therefore, there is a trade-off between the error rate (or T_g) and the data rate in the scheme.

3.3 Quadrant Division Based Motion Detection Algorithm

In the proposed MoC, we designed a quadrant division based motion detection algorithm. A flowchart of the quadrant division based motion detection algorithm is illustrated in Figure 3.6. Without loss of generality, it is assumed that the user creates one of the three exemplary motions. The algorithm detects the motions over the OCC link. For example, if the user makes a linear motion using a finger over a mobile phone camera, the centroids generated by tracking the motion are recorded as a line shape. It is important to note that this motion tracking is made possible, due to the illuminated finger that makes a clear distinction between the finger and the surrounding. The algorithm divides the screen into four quadrants based on the Cartesian coordinate system and counts how many quadrants the centroids are filled. For the linear motion, two quadrants are only required to be filled by the centroids. If the centroids are filled with more than two quadrants, then it will identify as other two possible shapes. As shown in Figure 3.6, if three quadrants are filled

with centroids, the motion is identified as an 'L'- shape, while if four quadrants are occupied by centroids then the algorithm goes through two stages for motion identification. For the present study, if the number of occupied quadrants is less than two, the motion is disregarded.

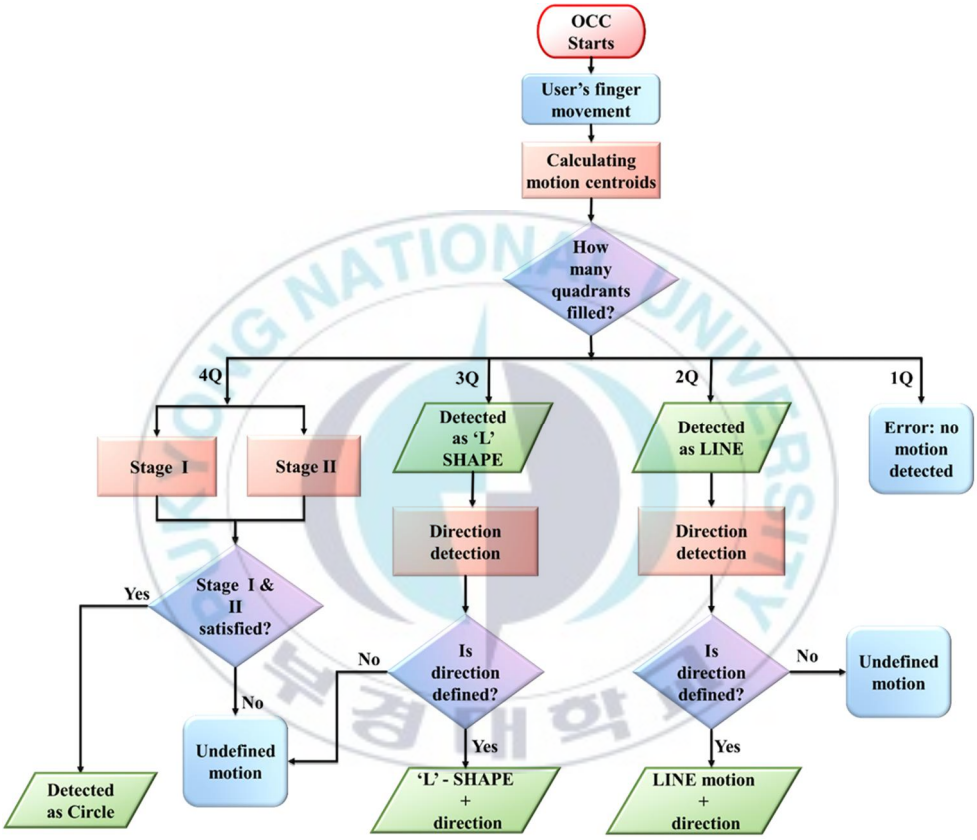

Figure 3.6. Flow chart of the motion detection algorithm.

In addition to identifying the motions, the algorithm identifies the direction of the motions. As shown in Figure 3.7(a), the principle of the direction

detection is based on the detection of the order of quadrant filling. Again, in the case of the line motion, the algorithm first identifies the shape of the motion and finds the order of the quadrant filling. As an example, if the centroids fill Q1 and then Q2 (Q1-Q2) or Q4 and then Q3 (Q4-Q3), it is defined as a left line. For the filling order of Q2-Q1 (or Q3-Q4), it is right line. The down and up lines are Q1-Q4 (or Q2-Q3) and Q4-Q1 (or Q3-Q2), respectively.

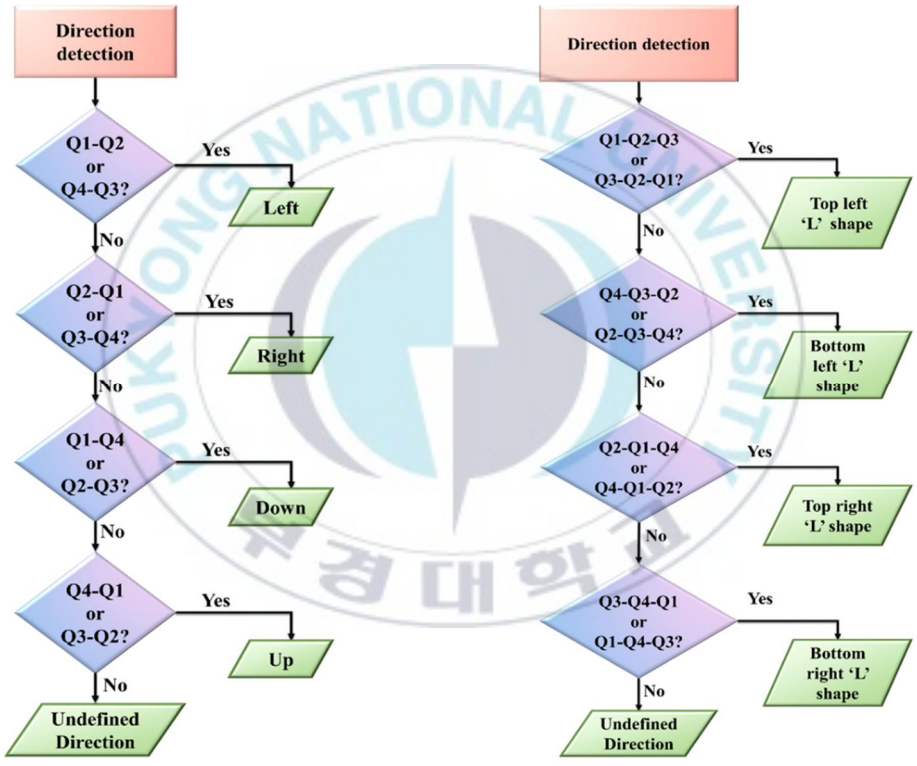

(a) (b)

Figure 3.7. Flow chart (a) Line shape with direction (b) L-shape with direction.

Similarly, for the ‘L’ - shape motion, three quadrants are expected to be filled with motion centroids. As in the line motion, the direction of the ‘L’ - shape motion can also be identified based on the direction in which the motion is performed. That is, for the ‘L’ - shape motion, if the centroids fill quadrants in the order of Q1-Q2-Q3 or Q3-Q2-Q1, it is defined as the top left ‘L’ - shape. Likewise, for the bottom left ‘L’, it would be Q4-Q3-Q2 or Q2-Q3-Q4. The top and bottom right ‘L’ – shape is detected if Q2-Q1-Q4 or Q4-Q1-Q2 and Q3-Q4-Q1 or Q1-Q4-Q3 are filled with centroids. This detection algorithm is illustrated in Figure 3.7(b).

As part of the further verification of the proposed algorithm for the motion detection, let us consider a circle motion that would be considered relatively complex to detect. We consider a two-stage detection process based on centroid distribution (CD) and the centre of centroid distribution (CCD). These two stages are also based on circle Hough transform (CHT) technique for defining the radii levels for circle detection as mentioned in [15]. CHT is a basic technique used in digital image processing, for detecting circular objects in a digital image. The detailed description is provided in Figure 3.8. Note that the CCD is the center of all the centroids distributed over four quadrants. The two-stage detection procedure is described below.

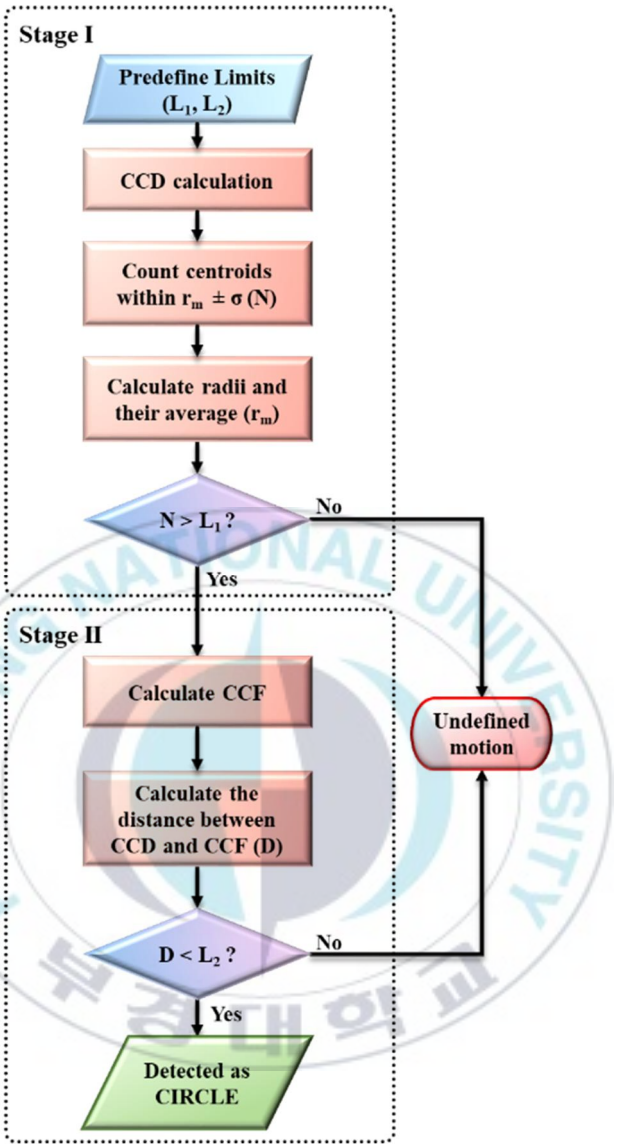

Figure 3.8. Flow chart of circle motion: Two-stage identification.

Stage I: The CCD is first found. The distance of each centroid to this CCD (i.e., radius) is then obtained. The average of the radii is then computed as r_m.

Considering the CD, some centroids significantly deviating from r_m can be discarded as they do not contribute to detecting the shape. To this end, we set a value of standard deviation (σ) so that the centroids within $r_m \pm \sigma$ are found. The number of centroids in this range, *N*, is then obtained. It should be noted that σ needs to be determined under the consideration of a perfect circle shape and an image frame size as adopted in the CHT [15]. The algorithm then detects the circle motion by comparing *N* with a predefined limit (L_1). If *N* is larger than L_1, it is determined as a detectable motion. The decision for the circle motion will be finally made in stage II.

Stage II: In this stage, the center of capture frame (CCF) is found. Obviously, the CCF is fixed as it is the center of the capture frame over which the motion is performed. The distance between the CCD and the CCF is calculated and denoted as D. It is true that D is expected to be very small for the circle motion. That is, if D is smaller than a limit (L_2), the motion is detected as a circle.

It is important to note that although the two-stage motion identification algorithm for the circle motion has been proposed with a view to allowing various circle motions that the user would make over the OCC, it can be reduced to a single-stage algorithm for simple and rapid detection. That is, the

algorithm with stage I only can also be applied for most circle motions, except for very irregular circles. In addition, it is certain that the proposed algorithm can be further extended to detect various other circle-like motions, such as arc, ellipse, and semicircle. One important aspect of motion detection based on mobile phones is the duration of motion. If the motion is performed very fast, the CD would be sparse, resulting in irregular distribution and subsequently undefined motion. In the current experiments, a suitable value of empirically obtained Δt is 4 s with a tolerance of ± 2 s. For obvious reasons, the motion duration (Δt) is subject to both the user and shapes. In addition, it can be limited by the capture rate of the camera.

3.4 Experimental setup

To verify the MoC in the OCC, an experiment was conducted with a mobile phone camera, an LED dot matrix and illumination LEDs. Figure 3.9 shows the experimental setup with the captured illuminated finger. For the purpose of demonstration of the proposed motion detection, experiments were performed at four different distances, that is, 12 cm, 15 cm, 18 cm, and 21 cm under a static condition. Similar to the transmitter employed in [11], we used an 8×8 dot matrix LED array with 4.31 V supply voltage and 10 illumination

LEDs with 3.143 V supply voltage and 60 mW optical output power. In addition, five different T_g values were used for the transmission, that is, 100 ms, 200 ms, 250 ms, 500 ms, and 1000 ms.

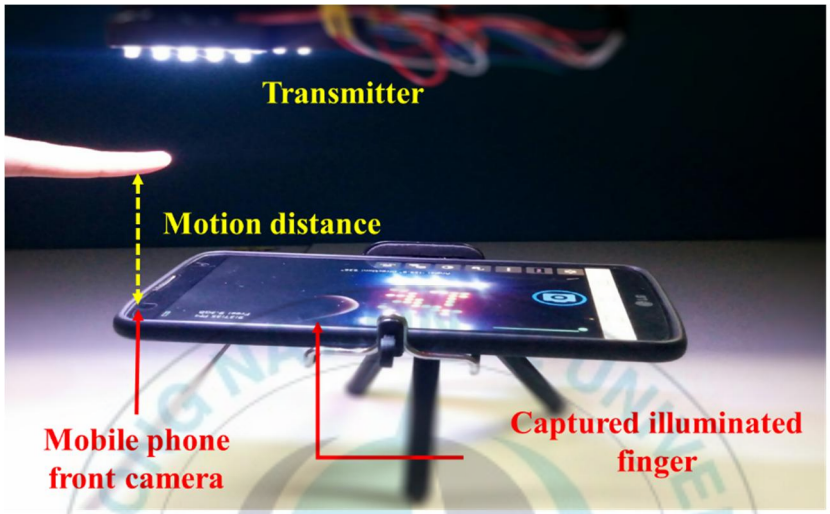

Figure 3.9. Experiment setup.

Motions and data were received on an Android mobile phone camera that has a resolution of 1920×1080 pixels with a capture speed of 30 fps. An optimum motion distance between the user finger and the mobile phone was found to be in the range of 7-8 cm for all considered transmission distances. When the user forms a motion, it is captured by the mobile phone camera in the form of a video.

For a mobile phone camera with a lower resolution, it would result in a smaller OCC distance, but the motion detection performance presented remains unchanged, due to the fact that the motion distance in the present experiments is still close enough to the camera. A higher LED illuminance level can certainly increase the transmission and motion distances. Likewise, a higher capture speed benefits dense motion centroids; thus, the success probability of motion detection can be increased. The high capture speed will also reduce the motion duration. Therefore, the present scheme can be designed to be more practically viable in accordance with camera features and light intensity.

3.5 Results and Analysis

Experiment results are shown in Figure 3.10 in which the centroid distributions are marked using red dots. These red dots represent tracked motion of user's finger. It is worth noting that these are representative results for three detected shapes, i.e., line, circle and ‘L’ - shape. The algorithm can detect the motion clearly and classify the shapes made by the user’s finger movement.

Based on the proposed algorithm, the frame for the motion detection is divided into four quadrants, and the detected motion is represented by centroid points (i.e., red dots). As the algorithm checks for the number of occupied quadrants, the motions are classified into line, L-shape, and circle. For the line and L-shape motions, the directions are also detected by finding the order of the quadrants filled. Figure 3.10 shows four different directions-up, down, right, and left line, and also top and bottom left and right L-shape motions. It should also be noted that the experiments were conducted for various types of circles to verify the robustness of the detection algorithm.

Since the OCC link supports communication as well as illumination, it is important to ensure that sufficient illuminance is provided in the first place. To this end, we measured average illuminance at the transmission distances of 12 cm, 15 cm, 18 cm, and 21 cm, and the values were found to be 2226 lx, 1533 lx, 1041 lx, and 721 lx, respectively. Thus, it was observed that the illuminance levels satisfy the illumination standard set forth by the International Organization for Standardization (ISO) [30].

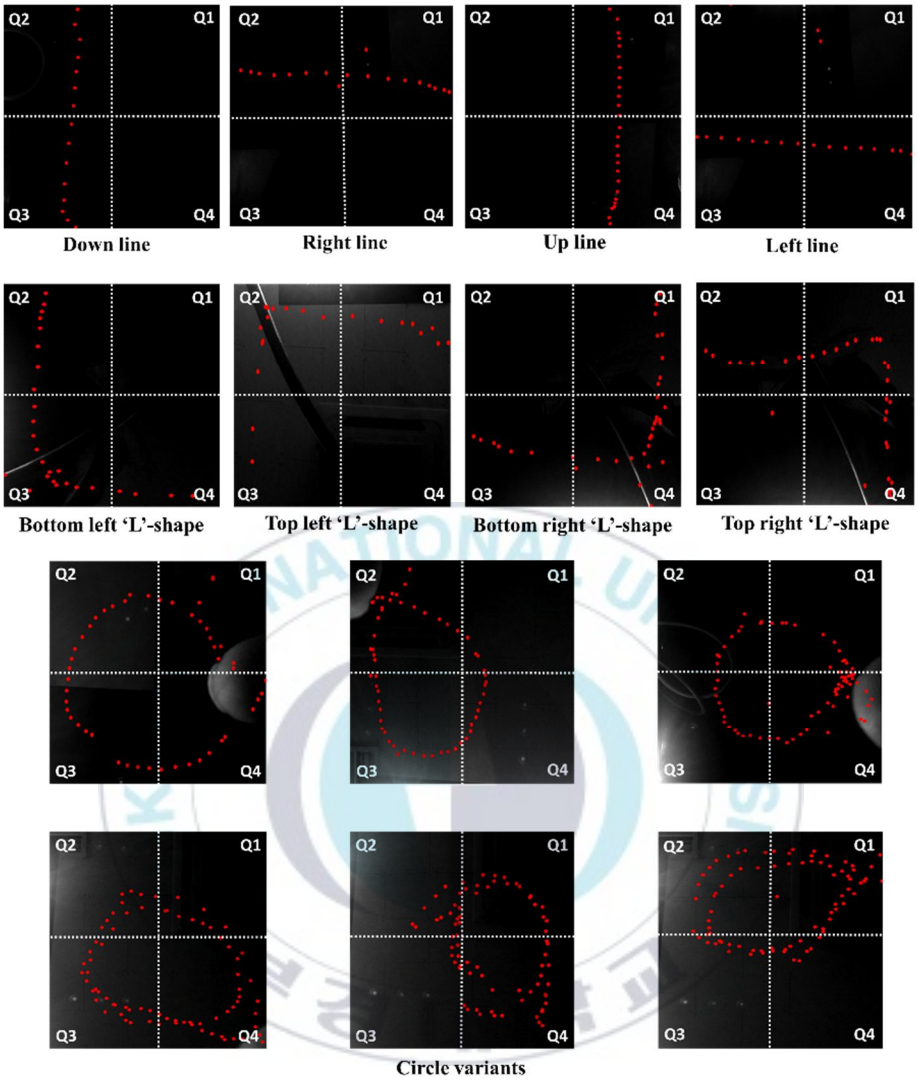

Figure 3.10. Experiment results: detected centroids of line, L-shape, and circle.

Table 3.1 shows the experiment results in terms of the percentage of success for the motion detection performed over a total of 90 experiments. That is, for each distance, 30 experiments were performed, 10 experiments per shape. In the experiments, the directions for the line and L-shape motions were also included. It is observed that the maximum percentage of success, 96 percent, was achieved at 12 cm distance. It is also found that the percentage of success decreases as the distance increases. Up to a distance of 18 cm, it was possible to detect the motion relatively accurately. For the 21 cm distance, however, the percentage of success was reduced to 76 percent. This is due to the fact that the illumination level of the finger becomes lower as it moves away from the illumination LEDs.

Table 3.1. Motion detection: Percentage of success.

Shapes	12 cm	15 cm	18 cm
Circle	10	9	8
L-shape	9	9	8
Line	10	10	9
Percentage of success	96%	93%	83%

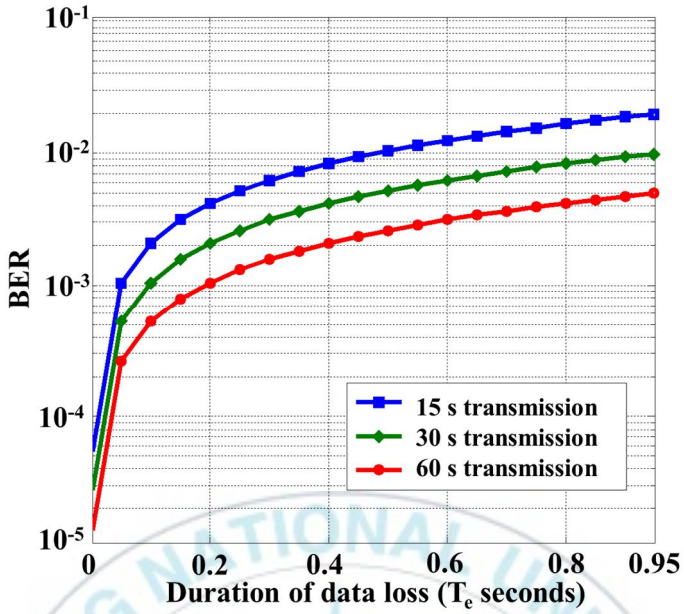

Figure 3.11. Performance analysis: BER

As noted previously, the proposed scheme is based on the periodic keyframe. It is interesting to analyze performance variation over the obstructed time during the user's motion. As we used an effective capture speed of 20 fps, the frame period is 50 ms. Figure 3.11 shows the bit error rate (BER) analysis in terms of T_e. It is observed that a longer data transmission produces improved BERs. This is due to the fact that the scheme can repeat the obstructed frames, thus improving the BER. For the 60 s transmission, an acceptable BER value of 10^{-3} was obtained at a T_e value of 0.2 s.

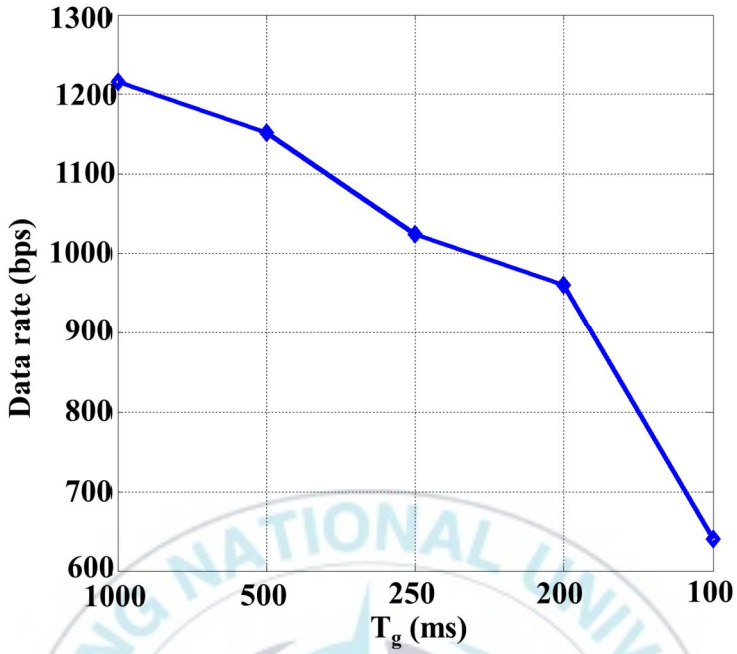

Figure 3.12. Performance analysis: Data rate.

The retransmission of obstructed frames would yield a lower data rate in the OCC. It is then worth analyzing the data rate relevant to T_g. Figure 3.12 shows the result. Note that the maximum achievable data rate in the current setting (no keyframes, 8×8 dot matrix LEDs, 20 fps) is 1280 b/s. In the current OCC-based MoC, the maximum data rate of 1216 b/s was achieved at a T_g value of 1000 ms. The reduction in the data rate is caused by the addition of the keyframe. It is evident that the smaller a T_g value is, the lower the data rate will be.

4. Neural Network Assisted Motion Detection

As previously mentioned in Chapter 3, the motion detection performance in OCC can be further enhanced using a concept of Deep learning-Neural Network for more practical implementation.

4.1 Neural Network

Artificial neurons based image and pattern recognition in a neural network (NN) has recently emerged as an efficient detection method, due largely to large-scale annotated datasets and the recent revival of deep convolutional NN [16][17]. In principle, the artificial neurons present in the hidden layers of the network receive multiple input samples to train the network. The training can be performed to optimize the network in terms of some fundamental criteria such as accuracy and robustness. In this way, the formation of complex detection algorithms can be circumvented. In this regard, some authors have studied an NN based indoor positioning technique in an OCC using the coordinate information [31].

In this study, a novel NN assisted motion detection scheme in optical camera communications (OCC) is proposed. As earlier described in Chapter 3, in the MoC in OCC, the motions are captured by a smartphone camera over

existing OCC links [9]. A unique motion detection algorithm was proposed, based on a complex yet efficient quadrant division method. The motion over camera scheme was capable of detecting and identifying the motions accurately over a motion distance of up to 8 cm and a transmission distance of 30 cm [9].

Motivated by the potential of the trained neurons in the NN, we propose a more practical and realistic motion over camera scheme over an OCC link. That is, as the motion performed by the user represents some pattern in the form of shape, trained neurons are employed to improve the performance of motion detection in terms of accuracy and transmission distance in the OCC. Therefore, the scheme can avoid the use of complex algorithms at the receiver to detect complex motions. Unlike previous image and pattern recognition schemes based on an NN aim to detect the patterns represented by images, the present motion detection scheme is based on the motion represented by data samples in the form of the *centroids*. In fact, the trained neurons based motion detection (TNMD) is due to the feature of the centroid data samples. By making use of trained neurons in the motion detection, the proposed TNMD is found to increase the motion distance up to 10 cm, while the transmission distance is extended up to 200 cm.

4.2 NN based Motion Detection

Figure 4.1 illustrates the block diagram of the proposed TNMD in the OCC. An 8×8 red, green, blue (RGB) LED array is used as the transmitter with four corner LED anchors for reference light metering and focus for the camera and with one synchronization LED for synchronization [11]. As the user performs a motion, the motion is captured in the form of a video. The motion is then expressed as centroids that represent the center of a moving object in the form of coordinates as mentioned in Chapter 3. These motion centroids obtained from the user's finger movement are fed to the pre-trained TNMD system where hidden and output layers are formed to detect and identify the motion performed by the user. For demonstration purposes, we consider seven motions created from two simple yet natural motions, i.e. line and circle.

A random binary data stream is generated by the data generation block in the transmitter. The on-off keying (OOK), which is the most commonly used modulation scheme for OCC, is employed for data modulation to transmit the data through each LED of the 8×8 RGB LED array. The data is mapped, according to the LED array addresses, and this mapped data is forwarded to the RGB LED array. In the receiver, the pre-trained TNMD system identifies the user's motion. Meanwhile, a demapping process entails the data

synchronization using the synchronization LED to extract the data from the received frames. An efficient differential detection threshold (DDT) scheme was used to accurately identify each LED in the array [11].

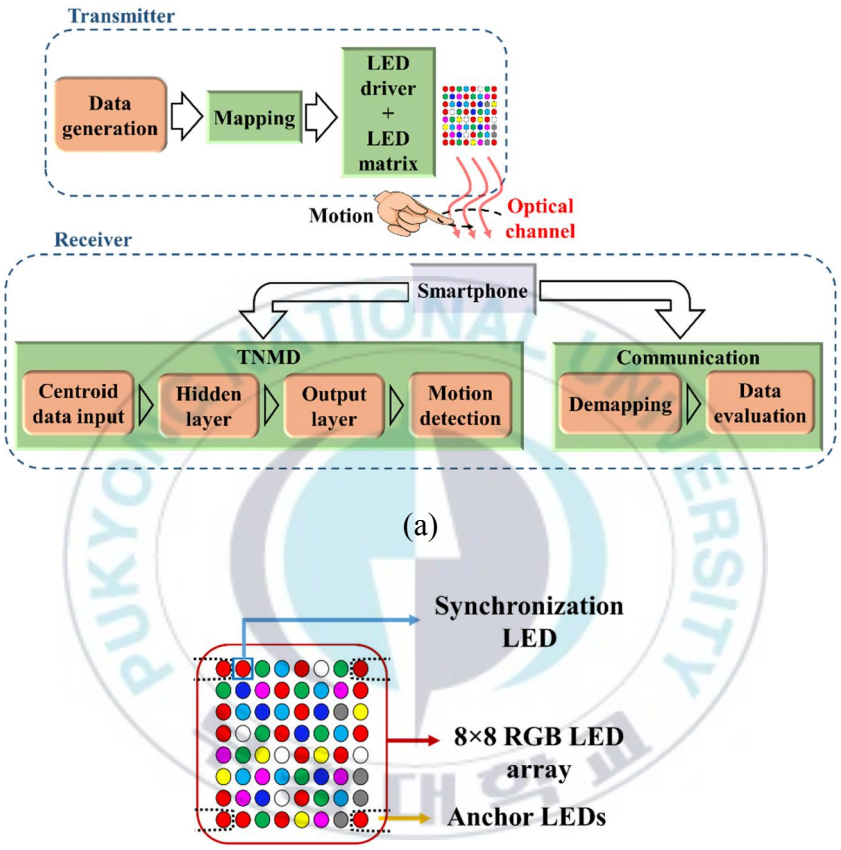

Figure 4.1. Proposed TNMD in the OCC: (a) Block diagram. (b) Transmitter design.

The transmitter consists of four anchor LEDs, one at each corner, and one synchronization LED at the top-left corner that is always in ON condition as shown in Figure 4.1(b). This synchronization LED is, however, only ON in the first frame of every group of N frames for time synchronization purpose. This first frame is denoted as F_s. While the motion detection is performed over an OCC link, it is apparent that the OCC link will be affected due to the obstruction caused by the motion. In the previous motion detection scheme in OCC [9], the data obstructed due to the motion was recovered based on the loss of keyframe. This may cause irrecoverable data loss when the data with no keyframe is obstructed. To address this issue, the present study employs the four anchors for alignment as well as for the detection of obstruction caused by the motion the user performed. Figure 4.2 depicts the data compensation method. The proposed data compensation process begins when any of the anchors is not detected in the receiver. To maintain communication quality, the data compensation process first discards respective damaged frames and requests retransmission via the receiver's repeat request. To detect the retransmitted data frames, F_{sr} is introduced as the header frame (synchronization bit) at the start of repeated frames.

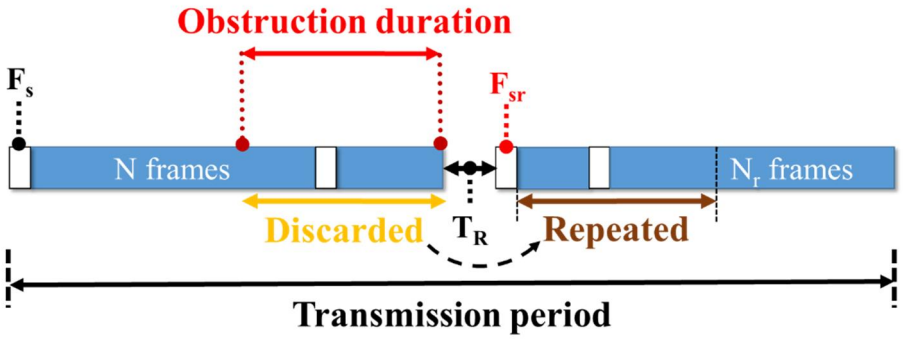

Figure 4.2. Transmit data compensation using anchors (N: number of frames, N_r: remaining frames, F_s: first frame, F_{sr}: header frame, T_R: delay due to repeat request).

In the event that F_s is not detected due to motion, the most recent group of N frames is discarded and repeated via the receiver's repeat request. N_r denotes the remaining frames that are stopped for the transmission due to obstruction. These N_r frames are then retransmitted after the repeated frames. It should be noted that some delay, T_R, is introduced in the retransmission of discarded frames due to the repeat request. Apparently, these anchors would reduce the data transmission rate slightly, because it occupies four data bits in every frame. That is, there is a trade-off between the bit error rate and the data transmission rate in the present scheme. It can, therefore, be said that the present scheme offers data compensation at the expense of reducing the data rate slightly.

4.3 Motion Detection Enhancement

The proposed TNMD aims to enhance the accuracy and efficiency of motion detection using the trained neurons in an OCC environment. Figure 4.3 shows the trained neurons structure of the TNMD system. This system is first pre-trained with the centroid data samples of predefined motions as the input and then utilized to identify the motion. The key principle of the TNMD is that since the system is designed to identify predefined motions only, the system can be pre-trained using the centroid data samples (obtained from the motion performed) to improve motion detection capability. Specifically, the feedback network is performed using a variable learning rate backpropagation algorithm for the training [32]. In the backpropagation algorithm, the output values are compared with the correct answer and then the error is calculated at the output and distributed back through the network layers. For the present study, the input for the training was 35 centroid data samples. That is, five centroid data samples for each of the seven predefined motions was employed. It is important to note that the training process for the TNMD is performed with the considered seven predefined motions only.

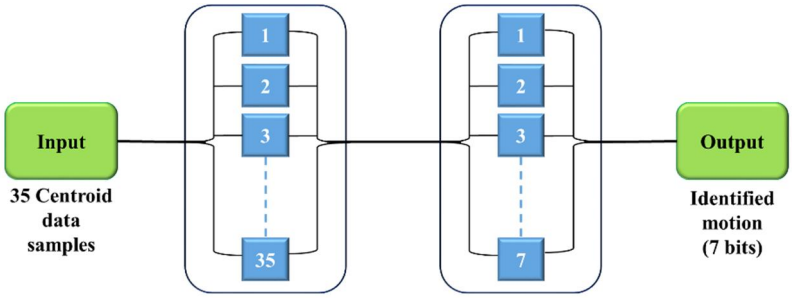

Figure 4.3. TNMD system overview: Trained neurons structure.

The pre-trained TNMD system is based on the NN where the input is 35 centroid data samples, a hidden layer comprised of 35 neurons and a hidden output layer comprised of 7 neurons. These neurons present in the hidden layers receive the 35 centroid data samples to produce the seven-bit output representing seven predefined motions. Prior to the measurements, the training goal was set to achieve zero error. To achieve this goal, the training phase was performed and reached the goal at 5000 training iterations (epochs) in a time window of up to four seconds. Figure 4.4 shows the training process that reached zero error at 5000 training iterations. The output of the training process is expressed in the form of training labels that are distinctive to each predefined motion.

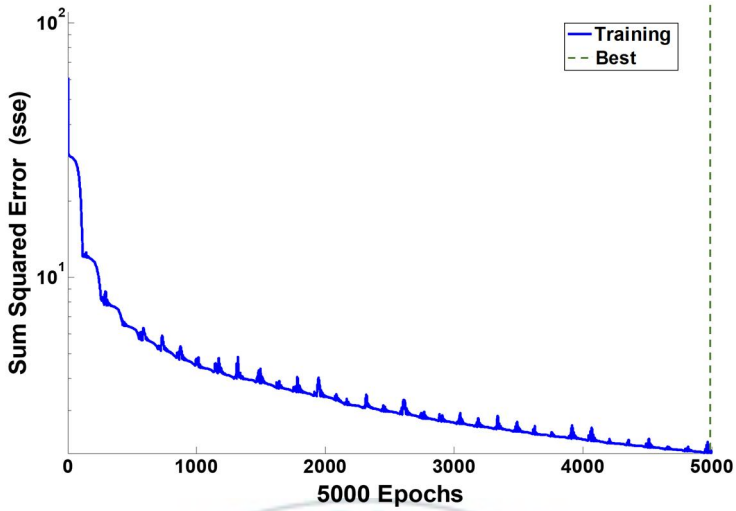

Figure 4.4. Training performance.

In general, it is worth noting that for a given number of input samples, the number of neurons in the hidden layers can be larger or smaller than the number of input data samples. However, if the number of neurons is unnecessarily large, it will result in a complex neural network, whereas a smaller number of neurons require more training iterations and processing time to achieve the predefined training performance. Therefore, there is a trade-off between the number of neurons and training complexity. As an example, although 35 neurons were employed in the current training, a smaller number of neurons, e.g. 20 neurons, can also be employed. Then, a total of 10000 training iterations, which is twice as many as the current 5000 iterations,

will be required with a processing time of up to nine seconds instead of four seconds in its training phase.

4.4 Experiment setup

Experiments were conducted to verify the proposed TNMD in the OCC. An Android mobile phone front camera with 1920×1080 resolution and 30 fps capture rate was employed as the receiver and an 8×8 RGB LED array with 20 Hz flickering rate as the transmitter. The frame period at the transmitter was set to 50 ms. Figure 4.5 shows an indoor experiment setup in a static condition with the captured LED transmitter as well as the illuminated user finger in the captured frame of the mobile phone front camera.

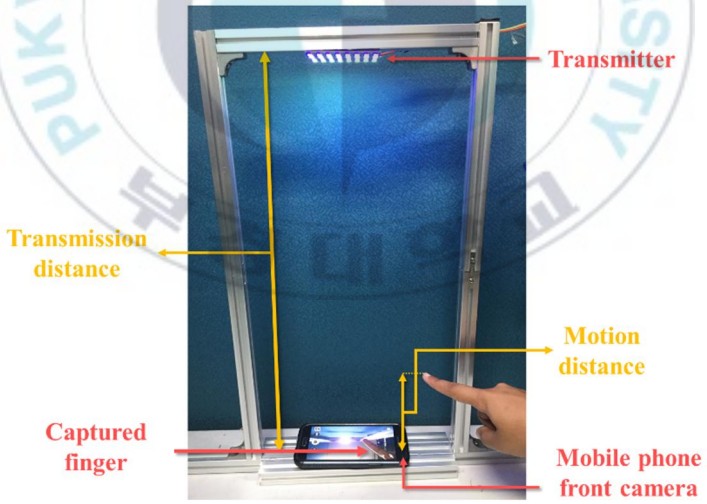

Figure 4.5. Experiment setup.

The experiments were conducted at a transmission distance of 25 cm with an increment of 25 cm under static conditions. For the current experiment setup, 225 cm was found to be the farthest distance for communication, while 200 cm distance was deemed the largest distance for motion detection. The distance limitations are due largely to the camera that is unable to capture the RGB LED array as the distance increases.

The motion distance, which is defined as the distance between the user finger and the camera, was found to be in the range of 7 cm to 10 cm for all transmission distances. However, it is obvious that these motion and transmission distances can be readily increased by increasing the LED illumination level and using higher capture speed cameras.

4.5 Results and Discussion

As previously noted, a total of seven motions were considered. Among these, semicircle, curve, circle and oval can be considered variant forms of circle, while vertical, horizontal and diagonal lines can be similar forms of line. These variants were purposely considered in the experiments to examine the robustness of the proposed motion detection scheme. The training process was performed with these seven motions. Figure 4.6 shows the experiment results.

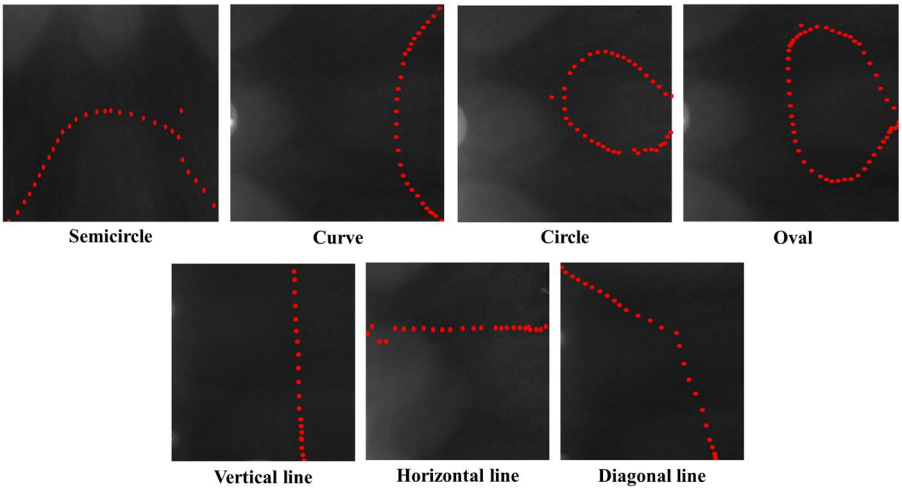

Figure 4.6. Experiment results: motion centroids for line and circle motion.

It is also important to ensure that sufficient illuminance is provided as the OCC link supports communication as well as illumination functionalities. Therefore, we measured average illuminance at each transmission distances of 25 cm up to 200 cm and the values were found to be 1560 lx for the nearest distance and 170 lx for the farthest distance. This measured illumination values satisfy the illumination standard set forth by the International Organization for Standardization (ISO) at a transmission distance of up to 75 cm, for which it requires an illumination level of 300 lx to 1500 lx in an indoor environment.

Table 4.1. Experiment results: TNMD accuracy.

Distance (cm)	100	125	150	175	200

Accuracy (%)	100	97	94	91	88

Table 4.1 shows the results of the motion detection accuracy in terms of percentage points at eight different transmission distances. As noted previously, the TNMD system is pre-trained with the centroid data samples of predefined motions as the input and then employed to identify the motions. The input to the TNMD system was 35 centroid data samples, a hidden layer comprised of 35 neurons and an output layer comprised of 7 neurons as shown in Figure 4.3. These centroid data samples were obtained from 35 experiments performed at eight different transmission distances. For each distance, 35 experiments were conducted, i.e., five for each motion. It is observed that the motion detection was perfect at a distance of up to 100 cm, but the detection became less accurate as the distance increased, due to the decrease in the illumination level. Nevertheless, the proposed TNMD was found to detect the considered motions relatively accurately at a transmission distance of up to 175 cm.

For the compensation of data loss due to the user's motion, four anchors were used, together with one synchronization LED in the 8×8 RGB LED array. Therefore, the data rate, R_d, can be calculated as [11],

$$R_d = N_L \times 3 \times L_{FR} - N_A \quad (4.1)$$

where N_L denotes the number of LEDs used for transmission, L_{FR} is a flickering rate of LED (20 pulses per second (pps) in the present scheme) and N_A is the number of anchors plus synchronization LEDs. It can be found that since the current experiment has four anchors each frame and one synchronization LED in the 8×8 RGB LED array, the maximum achievable data rate is 3.759 kbps.

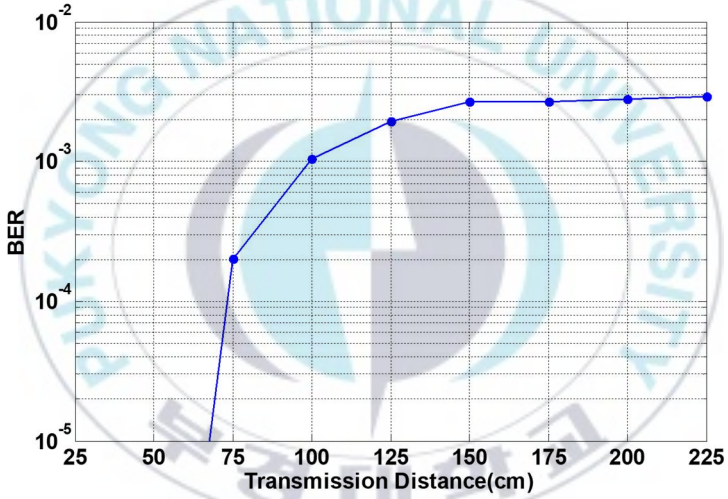

Figure 4.7. BER performance.

As the proposed TNMD ensures a short-range indoor communication as well as the motion detection, it is worth examining the communication quality in terms of bit error rate (BER). The data loss due to the user's motion is

recovered via the receiver's repeat request when any one of the four anchors is not detected at the receiver. Figure 4.7 shows the BER analysis. It shows no errors up to the transmission distance of 50 cm. An acceptable BER value of 2.6×10^{-3} was achieved at a transmission distance of up to 175 cm.

In conclusion, the proposed TNMD scheme that employs neurons in the NN at the receiver can significantly enhance the performance of motion detection functionality in the OCC. Unlike the conventional image-based NN schemes, the proposed TNMD scheme is based solely on centroid data samples rather than motion images. In the training process, representatives of the considered seven motions were fed into the neurons training. To verify the proposed scheme, it was experimentally evaluated in terms of its motion detection accuracy and communication quality. The experiment results demonstrate that the TNMD performs accurate detection with 35 centroid data samples, one hidden layer and one output layer at a transmission distance of up to 175 cm. In addition, an experimental data rate of up to 3.759 kbps was achieved. It is clear that the communication quality and transmission distance can further be improved with a larger illumination LED array, increased spacing between the LEDs, and advanced cameras with higher capture rates. The accuracy of the motion detection can also readily be enhanced with a

higher number of samples and layers of neurons. Therefore, the TNMD can be considered suitable to offer practical and convenient indoor smart home environments.

5. Selective Capture for V2V

As described in Chapter 1, the target of this study is to develop a high-speed, flicker-free and short-range OCC system under OWC. To increase the capture speed of camera receiver a novel technique termed as Selective Capture is implemented and analysed.

5.1 Flicker-free OCC

One of the major challenges in optical camera communication (OCC) is low data transmission rate, due to the low sampling rate of a camera-based receiver, compared with high-speed modulation of light emitting diodes (LEDs). Therefore, authors investigated the potential of increasing the OCC data rate with an array of LEDs used as the transmitter, in order to exploit an advantage of having a 2D space from the captured frames. In [11] authors utilized an array of single colored 64 LEDs and achieved an experimental data rate of up to 1280 bps. Recently, cameras with a color filter array over an image sensor have also become very common in smart devices, which opens up valuable opportunities to use red, green and blue (RGB) LEDs as transmitters and built-in cameras on smart devices as receivers [12]. The study assures that an image sensor is a natural massive-element and multi-color

receiver. Utilizing a single commercially available RGB LED and a standard 50-frame/s camera the experimental results showed a data rate of 150 bits/s over a range of up to 60 m [12]. Another OCC research developed a high data rate of 126.72 kbps using a not commercially available high capture rate camera of 330 fps and multiple intensity levels of colors to modulate [13].

For the basic purpose of illumination and data communication based on LED lighting, the data modulation at the transmitter must provide a wide range of dimming level and exhibit no flickering. To satisfy the flickering requirements of the transmitter in OCC, the flicker frequency should be greater than 100 Hz so that a typical human eye cannot respond to LED flickering when the frequency exceeds 100 Hz. The IEEE 802.15.7 VLC standard reported that the maximum flickering time period (MFTP) must be 5 ms (200 Hz) [5]. However, the commercial camera is limited to a capture rate of approximately 30/60 frames per second. As a result, the OCC itself can acquire signals at a very low sampling rate compared to the data transmission rate, resulting in a loss of unsampled data and poor signal detection probability. To control the flicker due to the limited frame rate of a commercial camera, an optical neutral density filter (ONDF) to attenuate the light and a field programmable gate array (FPGA) controlled digital camera was employed for

visible light positioning system [33]. However, the frame rate of 108 fps and modulation frequency of 54 Hz is lower than the MFTP [5][33]. The extra hardware utilization at the receiver would incur less cost-effective implementation in practice.

5.2 Selective Capture Scheme

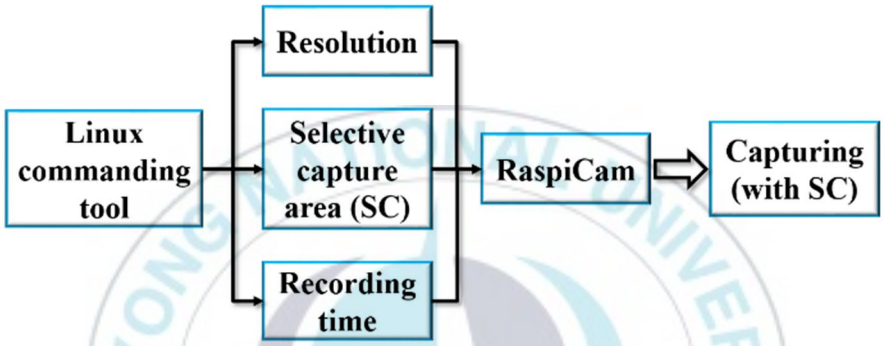

Figure 5.1. Selective capture scheme.

In this study, we propose a Selective Capture scheme (SC) to address an important issue of increasing the data transmission rate in OCC, i.e., high-speed OCC using SC. The camera receiver in OCC can be tweaked to capture the selected area only from the full camera capture frame, thus being termed as selective capture (SC). Unlike conventional OCC schemes, the proposed scheme performs the SC in the frame, not after the frames are captured. A Raspberry Pi camera module (RaspiCam) was used as the receiver in the

proposed scheme and was tweaked to capture the SC only, thus resulting in a higher data transmission rate in an OCC link.

This RaspiCam is connected to the Raspberry Pi 3 module B that uses the Linux operating system. Therefore, the Linux commanding tool is used to tweak the RaspiCam as shown in Figure 5.1, to selectively capture the selected area from the full capture frame. This involves a process of setting capture parameters such as the recording time of the video, the resolution at which the video is to be captured and the SC area.

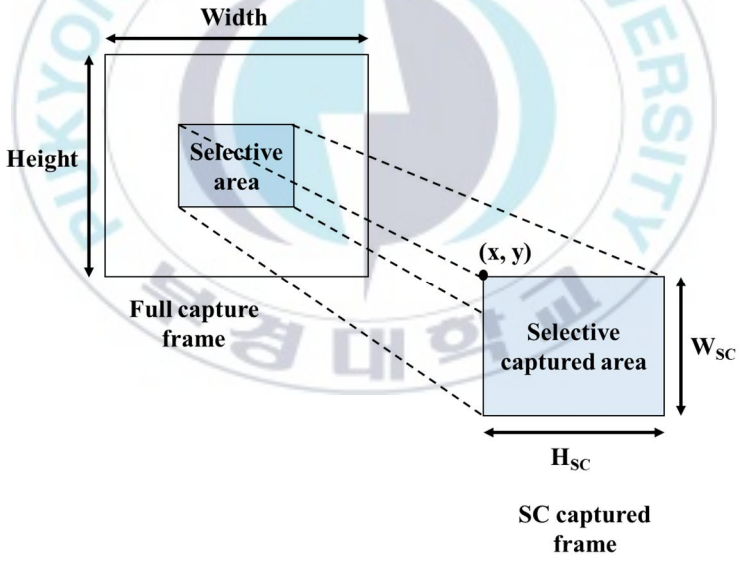

Figure 5.2. Selective capture concept.

Figure 5.2 illustrates the basic concept of SC scheme. The full capture frame is the frame captured using a normal (without setting SC) RaspiCam, while the SC captured frame is the frame captured by tweaking RaspiCam with SC value. The SC is set as follows:

$$SC = (x, y, H_{SC}, W_{SC}) \tag{5.1}$$

where x and y are the top right coordinates and H_{SC} and W_{SC} are the height and width of the SC capture frame.

5.3 V2V Communication in OCC

The widespread use of LEDs in traffic applications and the growing interest in intelligent transport systems (ITS) presents a number of opportunities for VLC and OCC applications. For example, LEDs are used for taillights, brake lights, headlights, and traffic signals. While the camera is considered as the receiver for automotive OWC systems [19][34]. Accordingly, vehicle-to-vehicle (V2V) and infrastructure-to-vehicle (I2V or V2I) communication systems using LED-based VLC and OCC technology have been studied [35][36]. To achieve a useful OCC system for automotive applications, much effort has focused on increasing data rate and communication distance by maximally utilizing spatial, frequency, intensity

or color dimensions. The barriers in OCC must be overcome: one is data rate improvement and another is accurate and quick LED detection. Recently, the optical vehicle-to-vehicle (V2V) communication system has been proposed employing LED transmitter and camera receiver [19][37]. The research employed a not commonly used high-speed optical communication image sensor (OCI) that provides capabilities for a 10 Mb/s optical signal reception [37].

5.4 Selective Capture for V2V Communication

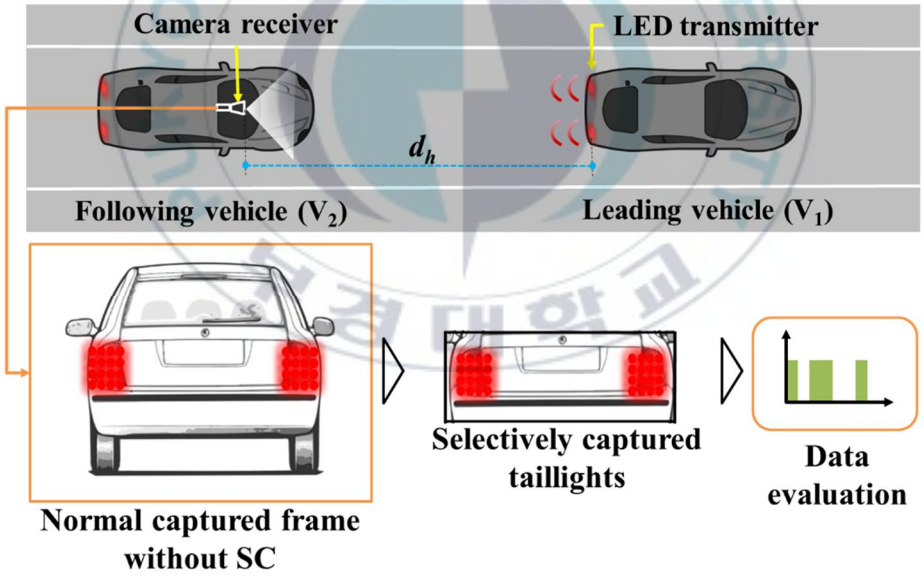

Figure 5.3. Proposed scheme: OCC for V2V using selective capture.

As previously mentioned, in the case of V2V communication there is need to establish high-speed communication. Therefore, we employ the SC scheme for high-speed and flicker-free OCC for V2V. The V2V communications can play an important role in enhancing vehicle safety by transmitting various internal as well as external data. Figure 5.3 illustrates the overview of the proposed OCC for V2V using SC. The vehicle LED light sources such as taillights or headlights of the V_2 can be used as the LED transmitter. In the proposed scheme, the camera used as the receiver is located at V_1. The V_2 can collect its own various internal data such as speed and traffic-related information and transmit it to the V_1 using the taillights as the transmitter.

Figure 5.4 (a) shows a block diagram of the proposed scheme. The proposed scheme employs a 4×4 red LED array representing the taillights of V_2 as the transmitter and a RaspiCam set with SC as the receiver located at V_1. The transmitter is comprised of the data generation block that generates random binary data for transmission along with its keyframe. The keyframe is a special header frame introduced in the generated data for evaluating the transmitted data in the receiver [9][11]. The most commonly used modulation scheme that is On-Off keying (OOK) modulation was employed for the data modulation to transmit data through each LED of the 4×4 red LED array. The

data mapping block maps the data according to the LED array addresses that are then passed on to the LED driver. The transmission through the optical channel is carried out by the 4×4 red LED array controlled by the LED driver. On the receiver side, data reception is carried out using the RaspiCam set with the defined resolution and the SC area using Linux commanding tool. Note that in the current scheme both the LED arrays transmit same data, therefore, redundancy is considered while evaluating the received data. The receiver also consists of a header image processing unit, a data image processing unit, and a demapping block. The captured image frames are fed to the header image processing unit, which identifies the LED array and detects the keyframe from the captured image frames. The demapping process performs time synchronization based on the detected keyframe and spatial synchronization to extract the data LED from the received frames. For the precise LED detection in the array on the OCC link, an efficient detection scheme called differential detection threshold (DDT) was employed [11].

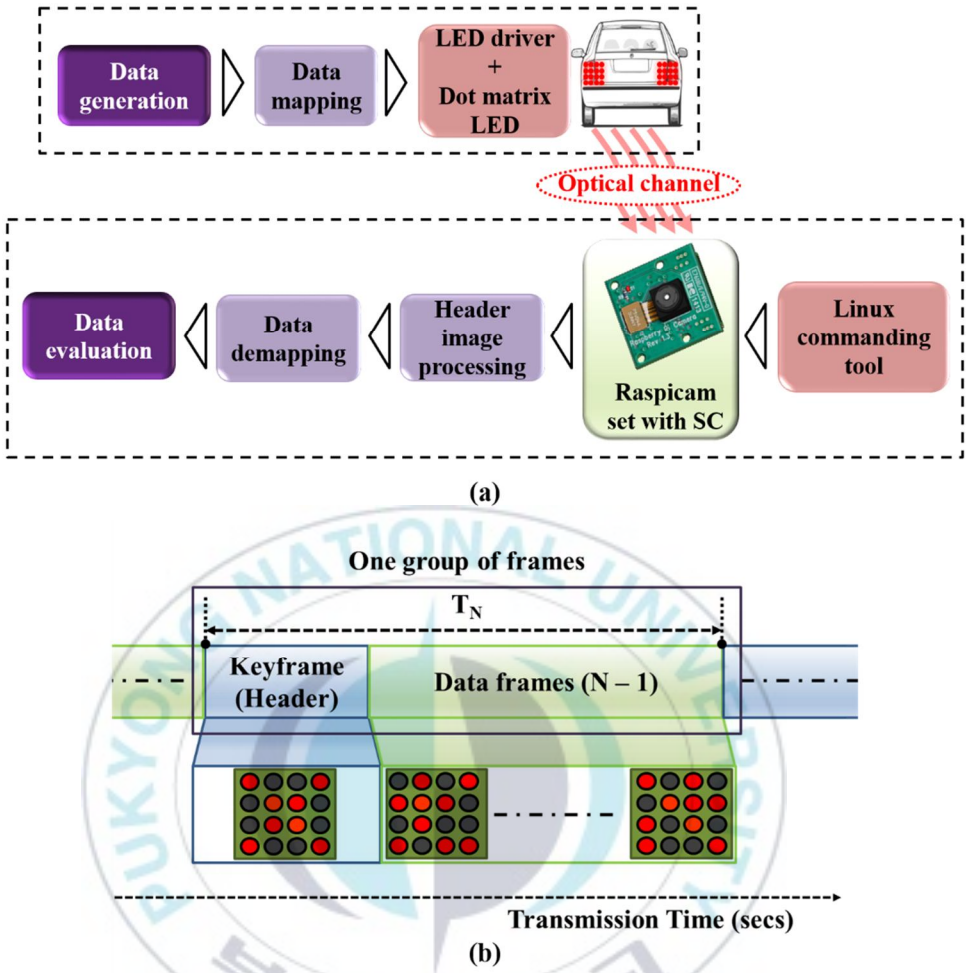

Figure 5.4. (a) Block diagram. (b) Keyframe configuration.

As described previously, a keyframe is added periodically in the transmitter as a header between every group of N frames. This keyframe plays an important role in performing the data synchronization. Figure 5.4 (b) shows the keyframe pattern used in the proposed scheme and keyframe configuration.

N denotes a total number of frames, and TN denotes the transmission time to transmit a keyframe and (N-1) data frames.

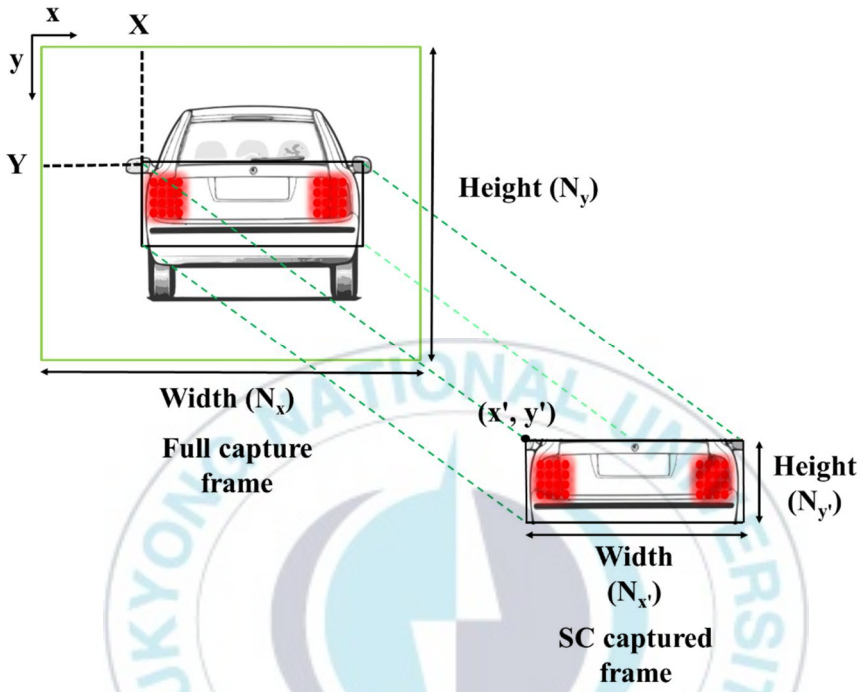

Figure 5.5. Concept of selective capture.

Figure 5.5 illustrates the concept of SC scheme performed by the RaspiCam to capture the taillights of the V_2 in V2V communication. The proposed optical camera based V2V communication is based on the SC of the RaspiCam which is used as the receiver located at V_1. The RaspiCam is connected to the Raspberry Pi 3 module that uses the Linux operating system. The Linux commanding tool is used to tweak the RaspiCam to selectively

capture as mentioned in [27] that involves a process of setting capture parameters such as the recording time of the video, the resolution at which the video is to be captured and the SC area.

The figure shows a full capture frame captured using a normal RaspiCam. While the SC frame is the part of the full capture frame which is selectively captured using the tweaked RaspiCam. The SC is set as follows:

$$SC = (x'; y'; Nx'; Ny') \quad (5.2)$$

where x' and y' are the top right coordinates and Nx' and Ny' are the width and height of the SC capture frame as shown Figure 5.5.

To set the SC area we utilized a well-known off-line image processing technique called template matching as mentioned in [38][39]. Template matching is a method to first determine the target template in the image, and then find the position of the target template in a frame image. The area similar to the template is determined as the target. In the present study, the template, i.e., the transmitter, is first selected from the image captured considering the minimum distance without any SC value set [38][39]. This selected template area is then used to track the transmitter in the full captured frame. The full frame is captured again at the minimum distance set according to the experiment and then it is compared with the template image using template

image traverse to find the most likely template, i.e., the position of the template in the full frame [39]. This position is then set as the SC value for tweaking the RaspiCam in the current scheme. The equation to calculate the SC value based on template matching technique is as follows [39], equation

$$SC = \sum_{x'=0}^{N_{x'}} \sum_{y'=0}^{N_{y'}} \left(T(x', y') - I(X + x', Y + y')\right)^2 \quad (5.3)$$

Assuming that the size of the template T is $N_x' \times N_y'$ (width×height), the size of the input image (full capture frame) I is Width×Height. The coordinate of one point in the template (SC frame) is *(x'; y')*, the pixel value of the point is *T(x'; y')*, the coordinate of the overlapping point is *(X + x';Y + y')*, which the pixel value is I *(X + x';Y + y')*. The coordinates *(X, Y)* are the origin of the template image on the full captured image (without SC). As mentioned previously, the template matching technique was performed by considering the nearest transmission distance by capturing the full capture frame (without SC) to evaluate the SC area. This value of the SC obtained from Eq. (2) is set for RaspiCam to capture the taillights of the V_2 at each distance. Note that in the current scheme, due to camera limitations, one SC value considering the nearest distance is set for all the transmission distances assuming that sufficient margin is provided for the near and the farthest distance.

5.5 Experiment setup

Figure 5.6 illustrates the experiment setup. Experiments were conducted indoor under an ambient light condition to verify the proposed OCC for V2V using SC scheme. The RaspiCam was employed as the receiver and two 4_4 red LED arrays as the transmitter (taillights) as shown in Fig. 5. Even though both the LEDs transmit same data, experiments were conducted to capture both the LEDs within the SC area so as to leave the margin for the movement of the car.

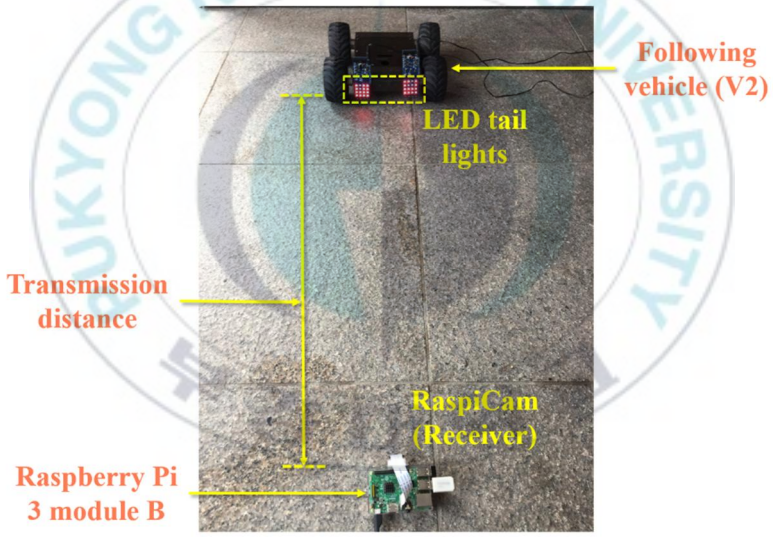

Figure 5.6. Experiment setup.

For the ease and convenience of the measurement campaign, the experiment setup was configured to represent a 1:4 scaled down representation

of a real transmission distance between vehicle taillights to RaspiCam. It is believed that this scale down experiment would not cause any adverse effect on the results. Experiments were performed at different transmission distances, i.e., 50 cm up to 225 cm with different SC values ranging from 0.0 to 1.0 in terms of pixels. For example, the SC value can be set to 0.3×0.9×0.3×0.9 pixels. Note that in the present scheme due to RaspiCam hardware limitations, the SC can only be limited in the range of 0.0 to 1.0 pixels for each transmission distance. As previously mentioned, both the LED arrays transmit the same data, therefore, they use same flickering rate.

Table 5.1. Experiment parameters.

Parameters	Values
Capture Device (RaspiCam)	5 V, 1.8 Amp
Raspberry Pi 3 module B	Third generation Raspberry Pi, 1 GB RAM
Resolution	640×480
Capture Rate	435 fps
Transmission Distance	50 cm to 225 cm
Red 4×4 LED array	12 V (supply voltage)
LED flickering rate	217 Hz
SC values	0.0 to 1.0 pixels

A light meter was used to measure light intensity which accuracy level is ±0.5 lux with a sampling period of 1sec. The measured light intensity was 800 lux at the minimum transmission distance of 50 cm and 150 lux at the maximum transmission distance of 200 cm on average and also measured ambient light illuminance incident from surrounding indoor walls is approximately 3 lux (±0.5 lux). Table 5.1 shows the key parameters for the experiment setup.

The data transmitted through the transmitter was received by a RaspiCam installed on the Raspberry Pi 3 module B board. As previously mentioned in the SC scheme, the resolution of the RaspiCam was set to minimum 640×480 pixels with same SC value for all the transmission distances. The current RaspiCam tweaked with SC values and minimum resolution can provide a capture speed of 435 fps. Therefore, the LED flickering rate was set to 217 Hz which satisfies the Nyquist theorem. According to the Nyquist's theorem, the sampling rate of the image sensor, which is the frequency at which a row of pixels is sampled, must be at least twice the rate of the highest signal frequency.

5.6 Results and Analysis

Figure 5.7 illustrates the experiment results for three different transmission distances, i.e., 50 cm the nearest transmission distance, 100 cm, and 200 cm the farthest distance. Note that as previously mentioned, the same SC value was set for every distance considering the nearest distance, i.e., 0.2×0.4×0.2×0.4 as shown in Figure 5.7. This is due to the fact that the SC value will be larger for the nearest distance and smaller for the longer distance. Therefore, it is necessary to ensure that the transmitter is captured even when the distance increases up to maximum viable distance.

The RaspiCam was first tested for a frame rate with respect to various values of resolution. Table 5.2 shows the variation in frame rate with respect to the change in the resolution of the RaspiCam. The maximum and minimum resolutions supported by the RaspiCam are 2592×1944 and 640×480 pixels, respectively. The same resolution values were tested with and without the SC scheme. It can be noted from Table II that the frame rate increases with the decrease in resolution as well is higher for each value of resolution when the RaspiCam with SC is employed, compared with conventional OCCs. The maximum achievable frame rate using SC was found to be 435 fps while the

one without SC was 120 fps at the minimum resolution value of 640×480 pixels.

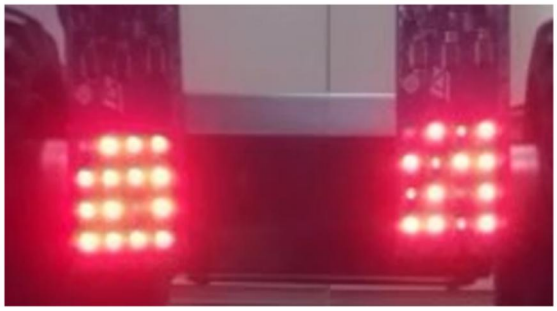

Transmission distance = 50cm, SC=0.2×0.4×0.2×0.4

Transmission distance = 100cm, SC=0.2×0.4×0.2×0.4

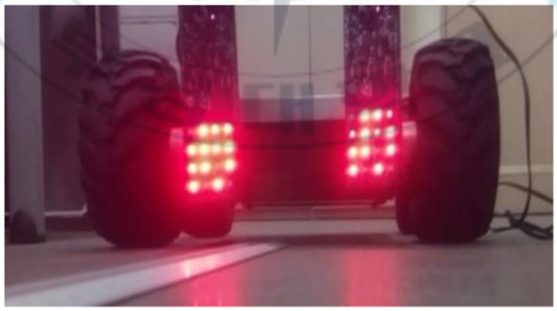

Transmission distance = 200cm, SC=0.2×0.4×0.2×0.4

Figure 5.7. Experiment results.

Table 5.2. Frame rate with respect to resolution.

Resolution	Frame rate (without SC)	Frame rate (with SC)
2592×1944	1 - 15	30
1920×1080	1 - 30	64
1296×972	1 - 42	140
1280×720	1 - 49	145
640×480	120	435

Similarly, the data rate with respect to the frame rate achieved with and without SC was also analyzed. The LED flickering rate was considered according to the Nyquist theorem. In the proposed OCC for V2V using SC (one keyframe, 4×4 red LED array), the maximum data rate of 3.456 kbps was achieved at 435 fps at the minimum resolution of 640×480 pixels as shown in Figure 5.8. The data rate, R_d can be calculated as [11],

$$R_d = N_L \times N_C \times L_{FR} \times KF \tag{5.4}$$

where N_L denotes the number of LEDs used for transmission, N_C denotes the number of colors used for transmission (one (red) in proposed scheme), LFR is a flickering rate of LED, which is 217 pulses per second (pps) in the present scheme and KF denotes the reduction of data rate due to the insertion of the keyframe over the transmission period.

Figure 5.8 shows the performance analysis of the data rate with and without SC with respect to the capture speed of the RaspiCam. It can be noted that the

OCC without SC can only achieve 944 bps data rate at 120 fps at the minimum resolution of 640×480 pixels using the same keyframe and transmitter configuration.

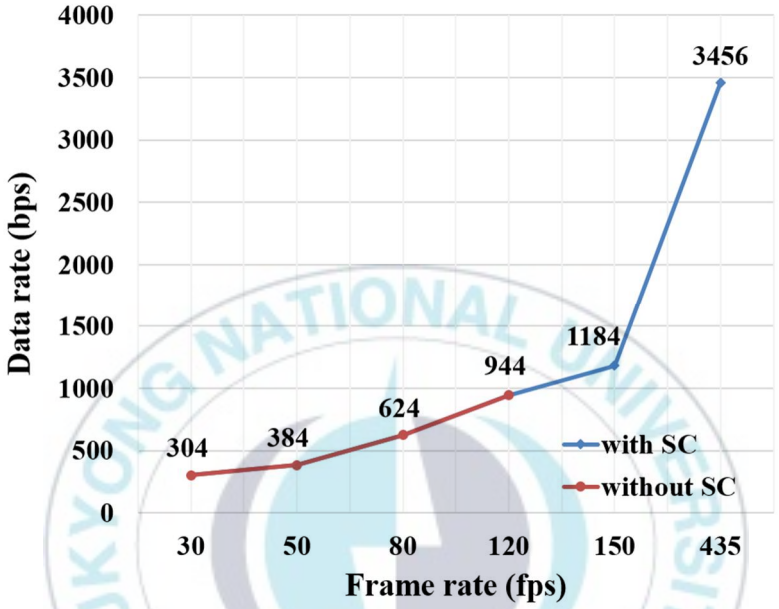

Figure 5.8. Performance analysis: Data rate.

Figure 5.9 shows the bit error rate (BER) analysis with respect to the transmission distance. The maximum capture speed of 435 fps at the minimum resolution of 640×480 pixels and indoor ambient light, was considered for the BER analysis. The results reveal that an acceptable BER value of 10^{-4} was achieved at a transmission distance of 125 cm.

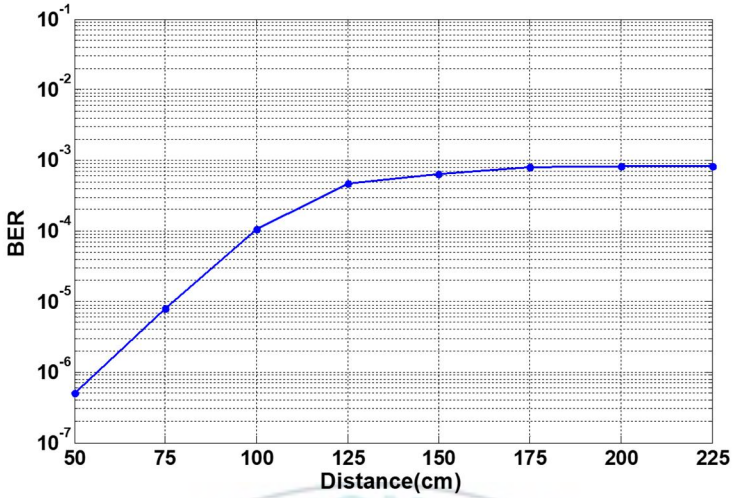

Figure 5.9. BER performance.

6. Conclusion

In this thesis, a convenient and cost-effective smart home environments based on motion detection in OCC is studied. The studies have conducted two major experiments individually, for both motion over camera and neural network assisted motion detection. The proposed camera based motion detection is attractive to various indoor applications, such as smart device control along with the data transmission through an LED-camera link.

The thesis also introduces a new camera capturing strategy called selective capture (SC) to achieve a high-performance and flicker-free OCC for V2V. The SC technique can enhance the data transmission rate, while providing a flicker-free transmission with the RaspiCam tweaked for SC.

In the first study, an efficient camera-based motion detection scheme in OCC has been presented. The motion detection is considered as a new additional functionality along with two usual functionalities: illumination and communication. The quadrant division based motion detection algorithm has been proposed, which detects the motion from the user who performs on a mobile phone and provides a decision. The algorithm could be enhanced for various other motions with some modifications. In the present work, assuming that the user performs a motion in a normal fashion, that is, within the motion

duration (Δt), nine different motions inclusive of all directions except for the circle motion are accurately distinguished. Simultaneously, the OCC communication quality was also analyzed and evaluated. The scheme ensures acceptable communication quality as well as sufficient illumination in an indoor environment. The experiment results demonstrate that a success probability of 96 percent and a data rate of up to 1216 b/s are achieved, while the OCC link is in operation. The proposed camera-based motion detection in the OCC can trigger a new dimension of OCC applications in a smart home or industry environment.

Secondly, the proposed TNMD scheme that employs neurons in the NN at the receiver can significantly enhance the performance of motion detection functionality in the OCC. Unlike the conventional image-based NN schemes, the proposed TNMD scheme is based solely on centroid data samples rather than motion images. In the training process, representatives of the considered seven motions were fed into the neurons training. To verify the proposed scheme, it was experimentally evaluated in terms of its motion detection accuracy and communication quality. The experiment results demonstrate that the TNMD performs accurate detection with 35 centroid data samples, one hidden layer and one output layer at a transmission distance of up to 175 cm.

In addition, an experimental data rate of up to 3.759 kbps is achieved. It is clear that the communication quality and transmission distance can further be improved with a larger illumination LED array, increased spacing between the LEDs, and advanced cameras with higher capture rates. The accuracy of the motion detection can also readily be enhanced with a higher number of samples and layers of neurons. Therefore, the TNMD can be considered suitable to offer practical and convenient indoor smart home environments.

A high-speed and flicker-free OCC for V2V communication using the SC technique has been presented. The proposed scheme aims to provide a flicker-free OCC for V2V communication by increasing the data transmission rate significantly using the SC technique. The RaspiCam receiver was successfully tweaked with the SC value evaluated by utilizing one of the well-known image processing schemes, i.e., template matching. This tweaked RaspiCam facilitated the selection of the resolution and the capturing of vehicle taillights as the selective area for communication between two vehicles. A maximum capture speed of 435 fps is achieved by the SC based RaspiCam at a minimum resolution of 640×480 pixels. Using this RaspiCam, we also achieve a data rate of up to 3.456 kbps, while a data rate of 944 bps is achieved without using the SC scheme. Therefore, it can be said that the proposed SC scheme in OCC

can increase the data rate nearly four times the data rate achieved by conventional OCCs. The scheme is found to be able to support reliable transmission at the farthest distance of 125 cm with a BER of 10^{-4}. It is worth noting that although a simple OOK modulation scheme was employed, more advanced modulation schemes and their variants can be considered for improved performance.

References

[1] C. X. Wang, F. Haider and X. Gao, “Cellular architecture and key technologies for 5G wireless communication networks,” *IEEE Communications Magazine*, vol. 52, no. 2, pp. 122-130, 2014.

[2] T. Nguyen, A. Aslam, T. Hossan and Y. M. Jang, “Current status and performance analysis of optical camera communication technologies for 5G networks,” *IEEE Access*, vol. 5, 2017.

[3] Y. Wang, X. Huang, J. Zhang, Y. Wang and N. Chi, “Enhanced performance of visible light communication employing 512-QAM N-SC-FDE and DD-LMS,” *Optics Express*, vol. 37, no. 3, pp. 15328-15334, 2014.

[4] A. Jovicic, J. Li and T. Richardson, “Visible light communication: opportunities, challenges and the path to market,” *IEEE Communications Magazine*, vol. 51, no. 12, pp. 26-32, 2013.

[5] IEEE Standard for Local and Metropolitan Area Networks-Part 15.7, “Short-Range Wireless Optical Communication Using Visible Light,” IEEE Standard 802.15.7, pp. 1-309, Sep. 2011.

[6] A. Sewaiwar, S. Tiwari and Y. Chung, “Visible light communication based motion detection,” *Optics Express*, vol. 23, no. 20, pp. 18769-18776, 2015.

[7] S. Tiwari, A. Sewaiwar and Y. Chung, “Color coded multiple access scheme for bidirectional multiuser visible light communication in smart home technologies,” *Optics Communications*, vol. 353, pp. 1-5, 2015.

[8] N. Saha, “Survey on optical camera communicaitons: Challenges and opportunities,” *IET Optoelectronics*, vol. 9, no. 8, pp. 172-83, 2015.

[9] S. Teli, W. A. Anugrah and Y. H. Chung, “Optical camera communication: Motion over camera,” *IEEE Communications Magazine*, vol. 55, no. 8, pp. 156-162, 2017.

[10] Y. M. Jang, “IEEE 802.15 WPAN 15.7 Amendment - Optical camera communications Study Group (SG 7a),” 13 8 2016. [Online]. [Accessed 13 8 2016].

[11] W. A. Cahyadi, Y. H. Kim and Y. H. Chung, “Mobile phone camera-based indoor visible light communications with rotation

compensation," *IEEE Photonics Journal*, vol. 8, no. 2, pp. 1-8, 2016.

[12] P. Luo, "Experimental demonstration of RGB LED-based optical camera communication," *IEEE Photonics Journal*, vol. 7, no. 5, pp. 1-12, 2015.

[13] W. Huang, P. Tian and Z. Xu, "Design and implementation of a realtime CIM-MIMO optical camera communication system," *Optics Express*, vol. 24, pp. 24567-24579, 2016.

[14] D. Ionescu, "A new infrared 3D camera for gesture control," in *IEEE International Instrumentation and Measurement Technology Conference, Minneapolis*, MN, 2310.

[15] L. Hong and Q. Yueliang, "Detecting persons using Hough circle transform in surveillance video," in *Proceedings in International Conference on Computer Vision Theory and Applications*, France, 2010.

[16] S. C. Hoo, "Deep convolution neural networks for computer-aided detection: CNN architecture dataset characteristics and transfer learning," *IEEE Transactions on Medical Imaging*, vol. 35, no. 5, pp. 1285-1298, 2016.

[17] J. Schmidhuber, “Deep learning in neural networks: an overview,” *Neural Networks*, vol. 61, 2015.

[18] H. B. C. Wook, S. Haruyama and M. Nakagawa, “Visible light communication with LED traffic lights using 2-Dimensional image sensor,” *IEICE Transactions on Fundamentals*, Vols. E89-A, no. 3, pp. 654-50, 2006.

[19] T. Yamazato, “Image-sensor-based visible light communication for automotive applications,” *IEEE Communications Magazine*, vol. 52, no. 7, pp. 88-97, 2014.

[20] S. Mitra and T. Acharya, “Gesture recognition: A survey,” *IEEE Transactions on Systems, Man, and Cybernetics*, Part C (Applications and Review), vol. 37, no. 3, pp. 311-324, 2007.

[21] R. Duda, P. Hart and D. Stork, Pattern Classification and Scene Analysis, New York: Wiley, 2000.

[22] R. C. Gonzalez and R. E. Woods, Digital image processing, Boston, USA: Addison-Wesley, 1992.

[23] N. Lalithamani, “Gesture control using single camera for PC,” in *Proceedings of International Conference on Information Security and Privacy*, Nagpur, 2015.

[24] L. Tianxing, A. Chuankai, Z. Tian, T. Andrew, T. Campbell and X. Zhou, “Human sensing using visible light communication,” in *Proceedings of the 21st Annual International Conference on Mobile Computing and Networking (MobiCom'15)*, New York, USA, 2015.

[25] S. Jennie, L. Huibao, and A. Glen, “Detecting regions of interest in images," *SPIE Newsroom*, 31 Nov. 2006.

[26] R. D. Roberts, “Automotive Comphotogrammetry," in *IEEE 79th Vehicular Technology Conference (VTC Spring)*, Seoul, pp. 1-5, 2014.

[27] S. P. Monacos, A. A. Portillo, W. Liu, J. W. Alexander, G. G. Ortiz, “A High Frame rate CCD Camera with Region-of-Interest Capability," in *IEEE Proceedings Aerospace Conference*, vol. 3, pp. 3/1513-3/1522, March 2001.

[28] S. Teli, and Y. H. Chung, “High-speed optical camera communication using selective capture," in *IEEE/CIC International Conference on Communications in China (ICCC)*, Qingdao, 2017 (in press).

[29] C. Danakis, M. Afgani, G. Povery, I. Underwood and H. Haas, "Using a CMOS camera sensor for visible light communication," in *Proceedings of IEEE OWC*, 2012.

[30] S. H. Chen and C. W. Chow, "Hierarchical scheme for detecting the rotating MIMO transmission of the indoor RGB-LED visible light wireless communications using mobile phone camera," *Optics Communications*, vol. 335, pp. 189-193, 2015.

[31] T. Komine and M. Nakagawa, "Fundamental Analysis for visible-light communication system using LED lights," *IEEE Transactions on Consumer Electronics*, vol. 50, no. 1, pp. 100-07, 2004.

[32] M. S. Ifthekar, N. Saha and Y. M. Jang, "Neural network based indoor positioning technique in optical camera communication system," in *International Conference on indoor Positioning and Indoor Navigation (IPIN)*, Busan, 2014.

[33] Q. Abbas, F. Ahmad and M. Imran, "Variable learning rate based modification in backpropagation algorithm (MBPA) of artificial neural network for data classification," *Science International*, vol. 28, no. 3, 2016.

[34] D. Li, W. Huang and Z. Xu, “Flicker free indoor visible light positioning system assisted by a filter and mobile phone camera,” in *IEEE/CIC International Conference on Communications in China (ICCC)*, Chengdu, 2016.

[35] T. Kasashima, “Interpixel interference cancellation method for road-to-vehicle visible light communication,” in *Proceedings of IEEE 5th International Symposium on Wireless Vehicular Communication*, 2013.

[36] S. H. Yu, O. Shih, H. M. Tsai, N. Wisitpongphan and R. Roberts, “Smart automotive lighting for vehicle safety,” *IEEE Communications Magazine*, vol. 51, no. 12, pp. 50-59, 2013.

[37] T. Saito, S. Haruyama and M. Nakagawa, “A new tracking method using image sensor and photo diode for visible light road-to-vehicle communication,” in *Proceedings of 10th International Conference on Advances in Communication Technology*, 2008.

[38] A. Takai, T. Harada, M. Andoh, K. Yasutomi, K. Kagawa and S. Kawahito, “Optical vehicle-to-vehicle communication system using LED transmitter and camera receiver,” *IEEE Photonics Journal*, vol. 6, no. 5, pp. 1-14, 2014.

[39] S. Iwasaki, M. Wada, T. Endo, T. Fujii, and M. Tanimoto, “Basic Experiments on Paralle Wireless Optical Communication for ITS," in *IEEE Intelligent Vehicles Symposium*, Istanbul, pp. 321-326, 2007.

[40] C. Xiu, and R. Wang, “Hybrid tracking based on camshift and template matching," in *29th Chinese Control And Decision Conference (CCDC)*, Chongqing, pp. 5753-5756, 2017.

List of Publications

Journal Papers

[1] **Shivani Rajendra Teli**, Willy Anugrah Cahyadi, and Yeon-Ho Chung, "Optical camera communication: Motion over Camera," *IEEE Communications Magazine*, vol. 55, no. 8, pp. 156-162 (2017).

[2] **Shivani Rajendra Teli**, Willy Anugrah Cahyadi, and Yeon-Ho Chung, "Trained neurons based motion detection in optical camera communications," *Optical Engineering*, (under review).

[3] **Shivani Rajendra Teli**, Willy Anugrah Cahyadi, and Yeon-Ho Chung, "Optical camera based high-speed V2V communication using selective capture," *IEEE Access*, (under review).

[4] Durai Rajan Dhatchayeny, **Shivani Rajendra Teli,** and Yeon-Ho Chung, "Optical extra-body communication using smartphone cameras for human vital sign transmission," *Wireless Communications and Mobile Computing*, (under review).

[5] **Shivani Rajendra Teli**, and Yeon-Ho Chung, "Selective capture based high-speed optical vehicular signaling system," *Signal Processing: Image Communication*, (under review).

Conference Papers

[6] **Shivani Rajendra Teli**, and Yeon-Ho Chung, "High-speed optical camera communication using selective capture" *in* 2017 International Conference on Communications in China (IEEE/CIC), Qingdao, Oct. 22-24, 2017.

[7] **Shivani Rajendra Teli**, and Yeon-Ho Chung, "Reflection based beam converging techniques for optical shadowing compensation in visible light communications" *in* Conference on Optoelectronics and Optical Communications Conference (COOC2016), Busan, South Korea, June. 1-3, 2016.

[8] Durai Rajan Dhatchayeny, Willy Anugrah Cahyadi, **Shivani Rajendra Teli,** and Yeon-Ho Chung, "A novel optical body area network for transmission of multiple patient vital signs" *in* 9th International Conference on Ubiquitous and Future Networks (ICUFN) 2017, Milan, 2017.

[9] Arsyad Ramadhan Darlis, **Shivani Rajendra Teli**, and Yeon-Ho Chung, "Water type identification in underwater VLC" *in* Full Symposium of the Korean Institute of Communications and Information Sciences, Busan, South Korea, 2016.

[10] Sudhanshu Arya, **Shivani Rajendra Teli,** Willy Anugrah Cahyadi and Yeon-Ho Chung, "UV propagation channel for non-line-of-sight optical communication," *in* the 6th International Conference on Green and Human Information Technology, Chiang Mai, Thailand, 2018 (Accepted).